City Research Online

City, University of London Institutional Repository

Typicality, Black Hole Microstates and Superconformal Field Theories

Vijay Balasubramanian[1,2], Bartłomiej Czech[1], Yang-Hui He[3],
Klaus Larjo[1] and Joan Simón[4] *

[1] *David Rittenhouse Laboratories, University of Pennsylvania,*
Philadelphia, PA 19104, USA

[2] *School of Natural Sciences, Institute for Advanced Study,*
Princeton, NJ 08540, USA

[3] *Merton College, OX1 4JD; Mathematical Institute, OX1 3LB, &*
Rudolf Peierls Centre for Theoretical Physics, OX1 3NP,
University of Oxford, UK

[4] *School of Mathematics and Maxwell Institute of Mathematical Sciences,*
King's Buildings, Edinburgh, EH9 3JZ, UK

February 2, 2008

Abstract

We analyze the structure of heavy multitrace BPS operators in $\mathcal{N} = 1$ superconformal quiver gauge theories that arise on the worldvolume of D3-branes on an affine toric cone. We exhibit a geometric procedure for counting heavy mesonic operators with given $U(1)$ charges. We show that for any fixed linear combination of the $U(1)$ charges, the entropy is maximized when the charges are in certain ratios. This selects preferred directions in the charge space that can be determined with the help of a piece of string. We show that almost all heavy mesonic operators of fixed $U(1)$ charges share a universal structure. This universality reflects the properties of the dual extremal black holes whose microstates they create. We also interpret our results in terms of typical configurations of dual giant gravitons in AdS space.

*vijay@physics.upenn.edu, czech@sas.upenn.edu, hey@maths.ox.ac.uk, klarjo@physics.upenn.edu,
J.Simon@ed.ac.uk

Contents

1   Introduction

Superconformal field theories (SCFTs) living on the world-volume of D3-branes transverse to the conical singularity of an affine cone over a Sasaki-Einstein manifold X are holographically dual to gravity on $\text{AdS}_5 \times X$. In this paper we explore the structure of heavy BPS states in these theories, describing their universal structural properties, and relating them to dual extremal black holes in $\text{AdS}_5 \times X$.

In [1], generating functions for enumerating mesonic BPS operators in these SCFTs were derived. This counting was extended to include baryonic operators in [2, 3], but in the present paper we consider only zero baryon charge. The authors of [1] derived the entropy associated to mesonic BPS states carrying a fixed linear combination of the three $U(1)$ charges. The most common and physically relevant example is states of constant R-charge R. In this article, we focus on toric cones and introduce a geometric construction that allows us to refine this counting and compute the entropy associated to any triple of charges rather than a fixed linear combination. By extension we are able to single out the particular triple that maximizes the entropy subject to any linear constraint on the charges. In particular this triple can be computed by finding the center of gravity of the pyramid cut of the dual toric cone by the constraint plane. Amusingly, this amounts to suspending the pyramid from a piece of string, providing a novel use for a different kind of string theory.

We will show that most heavy mesonic operators that are BPS have a universal structure. For a given set of $U(1)$ charges, we find the mean distribution of trace factors in heavy multi-trace operators. We then quantify the scale at which this distribution may be thought of as defining a typical structure for heavy operators, and spell out those features that are shared by almost all states. The heavy operators have gravity duals that can be interpreted in terms of giant gravitons [2] or in terms of dual giant gravitons [4]. This allows us to reinterpret our results as defining typical configurations of giant gravitons and dual giants. We also analyze the existence of horizons in the dual supergravity solutions.

The organization of the paper is as follows. In Section 2 we briefly review the connection between toric quiver theories and toric varieties. In Section 3 we present our geometric construction and compute the maximal entropy vector for any fixed linear combination of the $U(1)$ charges. We also show that the entropies found are not large enough to produce macroscopic horizons in the dual gravity description.

In Section 4, we treat the system statistically, and find the mean distribution of traces for the multitrace operators carrying any specified triplet of $U(1)$ charges. We also give the interpretation in terms of dual giant gravitons in AdS_5. Strictly speaking, since giant gravitons and dual giant gravitons are compact objects, their wavefunctions can spread over their moduli spaces. As we are analyzing these systems in terms of their typical classical configuration, it is important to evaluate how well the wavefunction localizes at a given point in the configuration space. For the special case of 1/8 BPS states in $\mathcal{N} = 4$ Yang-Mills theory, this analysis is carried out in Appendix B. In Section 5 we analyze the dual gravity description, and finally close in Section 6 with a discussion. In Appendix C we point out

some intriguing relations to topological strings and amoebae.

2 Review

The AdS/CFT correspondence has been extended to a set of type IIB string backgrounds of the form $AdS_5 \times X$, where X is a five-dimensional Sasaki–Einstein manifold [5]. The superconformal field theories dual to string theory on these backgrounds arise from a stack of D3-branes located at the conical singularity associated to the metric cone of X, and are quiver gauge theories. The material of the present paper applies to the most extensively studied class of the correspondence - when the cone over X is so-called **toric**.

Recently, there has been a realization that toric geometry, quiver theories, and dimer models give rise to an intimate web of relations. In this section we briefly review these connections; for a more comprehensive review the reader is referred to [6]. With these prerequisites, we devise a geometric construction in the dual toric cone to analyze BPS states carrying specified $U(1)$ charges. A well-known example of a toric Calabi-Yau cone is the complex cone over a complex surface known as the **first del Pezzo** surface [7]. Geometrically, this is the projective plane $\mathbb{CP}^2$ blown up at a point by a sphere. We shall refer to this Calabi-Yau cone as dP_1 and shall use this variety to illustrate this section and the ensuing discussions.

2.1 Toric quiver theories and planar quivers

A toric quiver theory consists of a set of gauge groups, $U(N_i)$ or $SU(N_i)$; for simplicity we take the groups to have equal rank: $N_i \equiv N$ for all i. Further, the theory contains a set of chiral superfields X_j, each transforming in the bifundamental representation $(N, \bar{N})$ under a pair of gauge groups and trivially under the others. The gauge groups and the matter can be presented in a directed graph, with gauge groups as nodes and matter multiplets as directed arrows between the two nodes under which the multiplet transforms non-trivially. The dynamics of the theory is encoded in a superpotential W. In toric quiver theories the form of W is highly restricted: it consists of a sum of monomials, with each field appearing linearly, and in exactly two terms with opposite signs. In Figure 1 we portray the quiver diagram and the superpotential of the quiver gauge theory corresponding to dP_1.

The toric quiver data and the superpotential can be incorporated into a single graph called the planar quiver. This is done by embedding the quiver into a torus, and "opening up" the arrows between the gauge groups in such a way that each arrow in the planar quiver corresponds to exactly one field. This can always be done so as to ensure that each term in the superpotential corresponds to a face in the planar quiver, i.e., for any face the arrows (fields) surrounding it make up a term in the superpotential. Each face is circled by the fields either in a clockwise or a counter-clockwise direction; the first corresponds to a negative and the latter to a positive superpotential term. See Figure 1 for the planar quiver of dP_1.

Figure 1: Left: The quiver diagram and the superpotential corresponding to dP_1. Right: The planar quiver

2.1.1 Mesonic operators in quiver theories

We are interested in multi-trace mesonic gauge invariant operators, which are of the form

$$O = \prod_{i=1}^{k} \text{Tr} \left(X_{b_{i1}} X_{b_{i2}} \ldots X_{b_{ia_i}} \right). \tag{2.1}$$

They form closed loops in the quiver and the planar quiver, with definite winding numbers (p, q) on the torus. The minimal mesonic operators are loops that pass through any node of the quiver at most once, i.e., operators that cannot be split into smaller components by adding traces. These generate the chiral ring of mesonic operators. Thus, any mesonic operator can be written as a product of these minimal loops *with suitably placed traces.*

The number of minimal operators can be computed from the quiver, but not all of these operators are independent: we must impose the vanishing of the F-terms coming from the superpotential W. Therefore, the minimal operators are split into equivalence classes under the F-flatness conditions $\partial W/\partial X_i = 0$. These equivalence classes are in one-to-one correspondence with the winding numbers on the torus, i.e., two operators are equivalent if and only if they share the same winding numbers (p, q).

Applying this to our example, from the dP_1 quiver of Figure 1 one can compute that there are 24 minimal loops, and in Table 1 we split these loops into 9 equivalence classes. Verifying that these are the equivalence classes under the F-term constraints is left as an exercise to the reader.

2.2 Brane tilings and dimer models

We can equivalently consider the graph dual to the planar quiver: this is obtained by replacing each vertex with a face, and each arrow with a perpendicular line. This dual graph

#	Minimal loops	Winding (p,q)
1	$X_{12}X_{23}^2X_{34}^1X_{41}^2$	$(-2,1)$
3	$X_{12}X_{23}^1X_{34}^1X_{41}^2$, $\quad X_{12}X_{23}^2X_{34}^1X_{41}^1$, $\quad X_{12}X_{23}^2X_{34}^2X_{41}^2$	$(-1,1)$
3	$X_{12}X_{23}^2X_{34}^3X_{41}^2$, $\quad X_{23}^2X_{34}^1X_{42}$, $\quad X_{13}X_{34}^1X_{41}^2$	$(-1,0)$
3	$X_{12}X_{23}^1X_{34}^3X_{41}^1$, $\quad X_{12}X_{23}^1X_{34}^2X_{41}^2$, $\quad X_{12}X_{23}^2X_{34}^2X_{41}^1$	$(0,1)$
6	$X_{12}X_{23}^1X_{34}^3X_{41}^2$, $\quad X_{12}X_{23}^2X_{34}^3X_{41}^1$, $\quad X_{23}^2X_{34}^2X_{42}$ $X_{23}^1X_{34}^1X_{42}$, $\quad X_{13}X_{34}^1X_{41}^1$, $\quad X_{13}X_{34}^2X_{41}^2$	$(0,0)$
2	$X_{13}X_{34}^3X_{41}^2$, $\quad X_{34}^3X_{42}X_{23}^2$	$(0,-1)$
1	$X_{12}X_{23}^1X_{34}^2X_{41}^1$	$(1,1)$
3	$X_{12}X_{23}^1X_{34}^3X_{41}^1$, $\quad X_{23}^1X_{34}^2X_{42}$, $\quad X_{13}X_{34}^2X_{41}^1$	$(1,0)$
2	$X_{13}X_{34}^3X_{41}^1$, $\quad X_{23}^1X_{34}^3X_{42}$	$(1,-1)$

Table 1: Equivalence classes of minimal loops and their windings for the dP_1 quiver.

is called a **brane tiling**. It has a natural bipartite structure, otherwise known as a **dimer model** [6]. If we color the nodes that correspond to negative superpotential terms in black, and those corresponding to positive ones in white, we see that each vertex is only connected to vertices of opposite color. See the brane tiling of dP_1 as an explicit example in Figure 2; note that we have marked the two nontrivial cycles on the torus and called them z and w.

The advantage of working with the brane tiling is that it allows us to find the toric Calabi–Yau manifold on the gravity side that is dual to the quiver gauge theory. This is accomplished using the Kasteleyn matrix K, which is formed from the brane tiling as follows.

First, we mark some edges in the tiling with minus-signs. This is done in such a way that for every face with (0 mod 4) edges surrounding it, an odd number of those faces have minus-signs; and for every face with (2 mod 4) surrounding edges, an even number have minus signs. This can always be done for any brane tiling. Then define the matrix elements K_{ij}, where the index i runs over the black nodes of the tiling, and j runs over the white nodes. K_{ij} is a sum over all the edges connecting the two nodes, with the following weights: -1, if the edge was marked with a minus sign above; z, if the edge crosses the cycle z in the tiling in the positive direction; z^{-1} if the edge crosses z in the negative direction, and likewise for w and w^{-1}. The positive direction when crossing the cycles z and w can be chosen arbitrarily, as long as it is consistently followed for all elements.

This is best illustrated by writing down the Kasteleyn matrix corresponding to the dP_1 brane tiling of Figure 2. In this case the minus-sign condition is satisfied if we choose the edge corresponding to the field X_{12} to come with a (-1). Then, denoting the black vertices 1,2,3 from left to right and denoting the white vertices 1,2,3 from bottom to top, we can write down the Kasteleyn matrix:

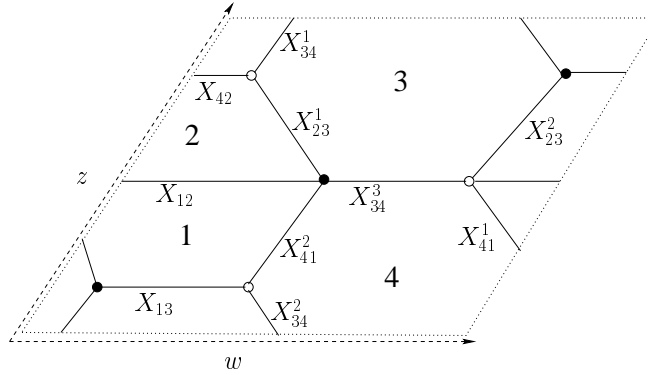$$K^{dP_1}(z,w) = \begin{pmatrix} 1 & z & w^{-1} \\ 1 & 1-z & 1 \\ w & 1 & z^{-1} \end{pmatrix}. \tag{2.2}$$

Figure 2: The brane tiling (dimer model) for dP_1.

2.3 Characteristic polynomial and the toric cone

Rather than K_{ij} itself, the object we really need is the determinant of K, which is the characteristic polynomial $P(z,w)$. Since $P(z,w)$ is a polynomial in two variables, each monomial $z^a w^b$ gives a point (a, b) in a two-dimensional lattice. These points make up a convex polygon called the **Newton polygon**, which in turn determines a toric variety. For details on the map between the toric variety and the toric cone we refer the reader to [8]. This completes the circle of correspondences. The beautiful fact is that this toric variety is precisely the singular Calabi-Yau cone to whose tip the stack of D3-branes is transverse by construction.

We embed the Newton polygon into the $z = 1$ plane[1] in $\mathbb{Z}^3$, and denote the boundary points of the k-gon by $\vec{v}_0, \ldots, \vec{v}_{k-1}$, ordered anti-clockwise around the polygon. Set $\vec{v}_k \equiv \vec{v}_0$. Linear combinations of the vectors $\vec{v}_i$ form the toric cone $\mathcal{C}$ of the variety; for details see again for instance [8]. For our long-running example, the del Pezzo quiver, the characteristic polynomial is

$$P^{dP_1}(z, w) = \det K_{ij}^{dP_1} = -4 + z^{-1} + w^{-1} + z + zw, \tag{2.3}$$

and the toric cone is shown in Figure 3.

In addition to the toric cone $\mathcal{C}$, we also need to work with its dual cone $\mathcal{C}^*$. The edges of the dual toric cone are generated by the interior pointing normal vectors to the exterior faces of the toric cone, normalized so that their magnitude is the smallest that can be achieved with integer components. In other words,

$$\vec{w}_{i,i+1} \propto \vec{v}_i \times \vec{v}_{i+1}. \tag{2.4}$$

---

[1] There is nothing special about the $z = 1$ plane: one can show that for a toric Calabi–Yau manifold the endpoints of the generators of the toric cone lie in a 2-plane, and without changing the variety one can perform a $SL(3, \mathbb{Z})$ transformation to map this plane to the $z = 1$ plane. Also note our abuse of notation: we label the coordinates on $\mathbb{Z}^3$ by (x, y, z), but this z is not related to the dummy variable z in the Kasteleyn matrix. As we will not utilize the Kasteleyn matrix beyond this point, we hope this does not cause any confusion.

$$v_1 = (-1, 0, 1), \quad v_2 = (0, -1, 1), \quad v_3 = (1, 1, 1)$$
$$v_4 = (0, 1, 1), \qquad v_5 = (0, 0, 1)$$

$$w_{12} = (1, 1, 1) \qquad w_{23} = (-2, 1, 1)$$
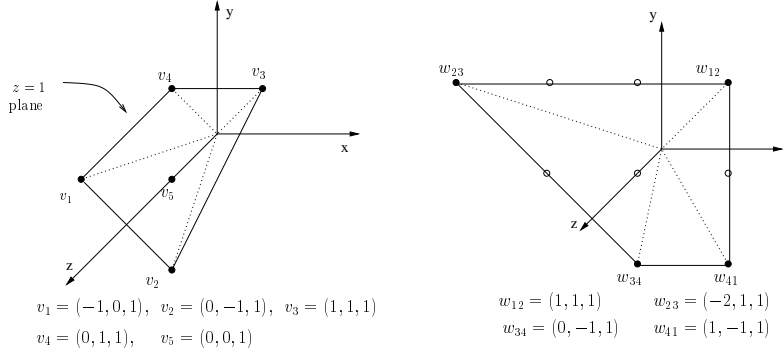$$w_{34} = (0, -1, 1) \qquad w_{41} = (1, -1, 1)$$

Figure 3: Left: The toric cone of dP_1. Right: The dual cone. The filled-in circles are the edge generators normal to the faces of the toric cone, and the empty circles are the remaining generators. Note that for this example the generators of the toric cone lie on a plane; this does not hold for a general toric variety, but only for Calabi-Yau ones.

To find the other generators of the dual toric cone, one simply needs to include the minimal set of interior points so that all the integral points in the dual toric cone are spanned by the generators. This is most easily illustrated by an example: in Figure 3 we plot the generators of $\mathcal{C}^*$ for the del Pezzo quiver, with filled circles for the edge generators, and empty circles for the interior points needed to complete the set of generators of the dual cone. The crucial fact that enables the counting of operators from toric data is that every integer point in the dual toric cone corresponds to a unique single-trace BPS operator [1].

Returning to our example, in Figure 4 we show the first three levels of points for the del Pezzo quiver. The single point on level 0 is naturally the identity operator. On level 1 the reader should compare the (x, y)-coordinates of the points with the winding numbers of operators in Table 1; they match perfectly. Clearly the higher levels will match as well, due to the conic structure of the construction.

Let us still flesh out this correspondence between points in the cone and operators by writing down the operator corresponding to point (x, y, z). This operator is given simply by

$$(x, y, z) \quad \leftrightarrow \quad A_{i_1} \dots A_{i_k}, \quad \text{with } w_{i_1} + \dots + w_{i_k} = (x, y, z), \tag{2.5}$$

where the A's are the independent minimal loops defined in Section 2.1, and w_i is the generator of the dual toric cone corresponding to the minimal loop A_i. Thus the correspondence above states that to construct the operator corresponding to the point (x, y, z), one has to choose a set of generators (minimal loops) such that the sum of these generators gives (x, y, z). There are generally many ways of choosing the loops so that this condition is satisfied, but the beauty of the construction is that all these operators will belong to the same equivalence class under the F-term constraints, which makes it possible to say that each point corresponds to a unique operator in the quiver.
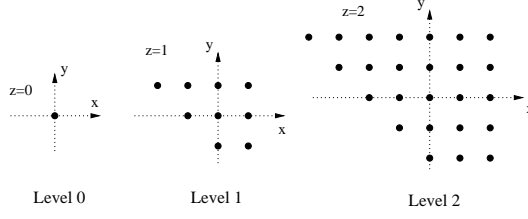
Figure 4: The first three levels of the dual toric cone of dP_1, i.e., the slices $z = 0, 1, 2$. Here the level counts the number of minimal loops.

2.3.1 Z-minimization and the Reeb vector

The final element we need is the Reeb vector $\vec{b}$ of the toric variety. Its significance is that it generates an isometry in the bulk geometry corresponding to the R-charge of the brane world-volume SCFT. Thus, in the dual toric cone, the Reeb vector is normal to planes containing operators of constant R. The directions generating an equal R-charge plane are then the remaining flavor charges [6], defined up to a residual $SL(2, \mathbb{Z})$. As shown in [9], the Reeb vector $\vec{b} = (b_1, b_2, 3)$ minimizes the volume cut from $\mathcal{C}^*$ by a plane $2(\vec{b}, \vec{n}) = 1$. This is equivalent to minimizing the quantity Z:

$$Z(b_1, b_2) \equiv \sum_a \frac{(\vec{v}_{a-1}, \vec{v}_a, \vec{v}_{a+1})}{(\vec{b}, \vec{v}_{a-1}, \vec{v}_a)(\vec{b}, \vec{v}_a, \vec{v}_{a+1})} \,, \tag{2.6}$$

where $(\vec{v}_i, \vec{v}_j, \vec{v}_k)$ is the 3×3 determinant constructed from the three column vectors. Z essentially corresponds to the Einstein–Hilbert action for a metric h on X, and thus minimizing it, i.e., finding the critical points, corresponds to finding the Sasaki–Einstein metrics for this action. In the above we set $b_3 = 3$, which holds in the $SL(3, \mathbb{Z})$ frame in which the Newton polygon is embedded in the plane $z = 1$. Thus finding the Reeb vector is reduced to an algebraic problem of minimizing a function of two variables. For dP_1, the minimization yields the Reeb vector

$$b^{dP_1} = (0, 4 - \sqrt{13}, 3). \tag{2.7}$$

If we assemble the three $U(1)$ charges of the BPS operator into a vector $\vec{n} \in \mathcal{C}^*$, then the value of the R-charge (and conformal dimension Δ) is given by its scalar product with the Reeb vector:

$$\Delta(\vec{n}) = \frac{3}{2} R(\vec{n}) = (\vec{b}, \vec{n}) \,. \tag{2.8}$$

Exemplary values of the R-charge for integer points in the dual toric cone of dP_1 are tabulated below. Notice that in general the R-charge of an operator need not be integer-quantized or even rational [10].

2.4 Toric cone as the phase space of dual giant gravitons

So far we have concentrated on the description of the half-BPS spectrum of mesonic scalar chiral primary operators $\mathcal{H}_{\mathrm{mesonic}}$ in $\mathcal{N} = 1$ SCFT quiver gauge theories. Our starting point

Level	Vector	Conformal Dimension
0	(0,0,0)	0
1	(a,1,1)	$7 - \sqrt{13}$
1	(a,0,1)	3
1	(a,-1,1)	$-1 + \sqrt{13}$
2	(a,2,2)	$2(7 - \sqrt{13})$
2	(a,1,2)	$10 - \sqrt{13}$
2	(a,0,2)	6
2	(a,-1,2)	$2 + \sqrt{13}$
2	(a,-2,2)	$2(-1 + \sqrt{13})$

Table 2: Conformal dimensions of charge vectors $\vec{n}$ in the dual toric cone of dP_1. The level denotes the number of minimal loops. The R-charge is independent of the first coordinate of $\vec{n}$ because $b_1 = 0$.

was the mathematical description of toric cones $\mathcal{M}$ over Sasaki–Einstein manifolds X probed by D3-branes. However, the half-BPS sector of the gauge theory Hilbert space may also be analyzed in terms of (dual) giant gravitons. In this analysis, the machinery of toric geometry is as useful as it is on the gauge theory side.

We recall that BPS mesonic sectors in SCFTs allow different physical interpretations depending on the amount of R-charge carried by the states. For states carrying order N^0 charge, these are interpreted as pointlike rotating gravitons; when the charge becomes of order N, they can also describe giant gravitons or dual giants. Classically, the first set corresponds to rotating D3-branes wrapping homologically trivial 3-cycles in the cone $\mathcal{M}$ over the base X; the second set describes rotating D3-branes wrapping a 3-sphere in AdS$_5$. This last approach was adopted in [4], where the authors showed that $\mathcal{M}$ has a natural interpretation as the phase space of the dual giant.

Using geometric quantization, the Hilbert space for the dual giant $\mathcal{H}_{dg}$ was found to be given by the space of holomorphic normalizable functions on $\mathcal{M}$. Since $\mathcal{M}$ is toric, it was further shown that this space is spanned by the elements of the dual toric cone $\mathcal{C}^*$. Thus, there exists an isomorphism between $\mathcal{H}_{dg}$ and the dual toric cone $\mathcal{C}^*$.

Since dual giants are mutually BPS, the N-dual giant states can be described by N indistinguishable quantum particle states. Hence the N-dual giant Hilbert space is simply the N-th symmetric tensor product

$$\mathcal{H} = \mathrm{Sym}^N \mathcal{H}_{dg}. \tag{2.9}$$

This fact allows to compute the partition functions of these systems. We will be interested in the grand canonical partition function for multi-dual states, which was found in [4] and agrees with the grand canonical partition function of the CFT presented in [1]. We will be analyzing these partition functions in Section 4, and interpreting the results both in terms of typical mesonic CFT operators, and in terms of typical configurations of dual giant gravitons.

Isomorphism of Hilbert spaces: Besides the isomorphism of Hilbert spaces described above, there exists a further one between the Hilbert space of giant gravitons and $\mathcal{H}$ [2]. This can be seen as follows.

The classical moduli space of giant gravitons is given by the set of polynomials of degree N in $\mathcal{M}$ subject to a set of constraints [2]

$$P(z_1,\, z_2,\, z_3) = c + c_i z_i + c_{ij} z_i z_j + \cdots = \sum_I c_I z_I\,. \qquad (2.10)$$

Following [11], the quantum Hilbert space for such giants $\mathcal{H}_g$ is spanned by the states

$$|c_{I_1},\, c_{I_2},\, \ldots, c_{I_N}\rangle\,. \qquad (2.11)$$

These states are holomorphic polynomials of degree N over the classical moduli space and are symmetric in the $\{c_{I_i}\}$. Thus, $\mathcal{H}_g$ is the symmetric product

$$\mathcal{H}_{\mathrm{g}} = \mathrm{Sym}\left(|c_{I_1}\rangle \otimes |c_{I_2}\rangle \otimes \cdots \otimes |c_{I_N}\rangle\right)\,, \qquad (2.12)$$

where each $|c_{I_i}\rangle$ represents an holomorphic function over the cone $\mathcal{M}$ with base X. This establishes the isomorphism between the Hilbert spaces of giant gravitons and dual giants.

We want to emphasize that this last isomorphism is captured by the combinatorial identity, a cornerstone of the plethystic program:

$$g_N(t,\, \mathcal{M}) = g_1(t,\, \mathcal{M}^N/S_N)\,, \qquad (2.13)$$

where $g_N(t,\, \mathcal{M})$ stands for the partition function of the gauge theory of N D3-branes probing $\mathcal{M}$, whereas $g_1(t,\, \mathcal{M}^N/S_N)$ stands for the partition function of a single D3-brane in the symmetric product $\mathcal{M}^N/S_N$.

The full discussion is summarized by the equality :

$$\mathcal{H}_{\mathrm{g}} = \mathrm{Sym}^N \mathcal{H}_{dg} = \mathcal{H}_{\mathrm{mesonic}}\,. \qquad (2.14)$$

We conclude that the partition function $g_N(t,\, \mathcal{M})$ counts half-BPS mesonic scalar chiral primary operators, *and* giant graviton states carrying a certain R-charge, *and* dual giant graviton states carrying the same R-charge.

3   Counting multi-trace operators

In the previous section we learned how each point $\vec{n}$ in the dual toric cone corresponds to an operator in the quiver theory via (2.5). These operators are not gauge invariant as each field transforms in a non-trivial representation under two of the gauge groups. In order to create gauge invariant operators we need to contract appropriately the indices on the fields X_i. This can be done by inserting traces at appropriate places in the operator.[2]

---

[2] By constructing gauge invariant operators using traces we are picking a preferred basis that is convenient for us and which is related to multi-particle states in AdS space. Another possible choice for constructing such operators would be to use determinants and sub-determinants which are related to D-branes in AdS space.

The simplest way of making the operator in (2.5) gauge invariant is to take the trace of the entire quantity. This leads to a single-trace operator, which corresponds canonically to a point in the dual toric cone. As mentioned below eq. (2.5), this correspondence is bijective and extends to all the integer points in $\mathcal{C}^*$. Therefore every integer-coordinate point in the dual cone is uniquely associated with a single-trace gauge invariant operator. However, we can also create a gauge invariant operator by distributing several traces in the product (2.5) to produce multi-trace operators of the form (2.1). This may clearly be done in a multitude of ways. In this section we will compute the number of such inequivalent trace structures. This is important because for large charges the corresponding field theory states are expected to be dual to black hole microstates, and our computation of the degeneracy of operators for any triplet of charges provides a prediction for the entropy of these black holes. We return to this in more detail in Section 5.

Before proceeding, we should explain how our counting differs from the one done in the plethystic program [1, 3]. There, the authors computed the entropy of mesonic operators of a given R-charge and provided an implicit expression–the refined plethystic exponential– counting operators at any given *point* in the dual cone (meaning operators of a given R-charge and flavor charges n_1 and n_2). In this paper, we pursue a different strategy, which involves introducing a new slicing of the dual toric cone. This method affords an elegant geometric interpretation, and, crucially, allows us to find the *asymptotics* of the *refined* counting, which was not done in the plethystic program. As one expects the flavor charges of black holes to be measurable to classical observers, it is the refined counting carried out in this paper that is expected to match the entropies of the dual black holes.

There is a simple way of stating our counting problem: since each trace component in the expression (2.1) is a single-trace operator, it corresponds to a point in the dual toric cone. Thus, computing the number of ways of distributing traces is equivalent to finding the number of partitions of the vector $\vec{n}$ into components: $\vec{n} = \sum_j \vec{m}_j$. The asymptotics of this type of counting problems can be tracked using a theorem due to Meinardus [12]; our application of Meinardus' theorem will follow that of [1]. We shall proceed in the following steps: First, we count the number of partitions for all vectors on a fixed plane; this is equivalent to counting multi-trace operators with a single fixed charge, say R-charge. We then go on to count the vectors on this plane individually; this is the refinement, wherein a particular triplet of $U(1)$-charges is fixed. We carry out the computation in this way because, as we shall see in the ensuing arguments, this method leads to a handy geometric construction involving centers of gravity of certain pyramids.

3.1   Step 1: Partitioning co-planar vectors

As the first step we shall reproduce the non-refined plethystic counting, and use the Meinardus theorem [12] to find the asymptotic number of multi-trace operators on any plane of rational slope containing the point $\vec{n}$ in the dual toric cone. Let us pick such a plane and denote it by p. Then consider an auxiliary family $\{p_m\}$ of planes parallel to p, such that (1)

11

each point in the dual cone is contained in one of the planes, and (2) the planes are evenly placed, i.e., the distance between any two neighboring planes is fixed. In this auxiliary family we index the planes from the tip of the cone, and take $p_n \equiv p$ to be the plane that contains the point $\vec{n}$.

To illustrate this, we display a two-dimensional analogue in Figure 5; here the cone is chosen to be the positive quadrant of $\mathbb{Z}^2$, and parallel planes are drawn as parallel lines. Next we wish to find the sum of the number of different vector partitions (which we will call the *multiplicity*) of all the points on the plane p_n. This is the first step on the way to finding the multiplicity of the point $\vec{n}$. As is clear from the above setup and Figure 5, this problem is equivalent to enumerating the sets of vectors $\{\vec{m}_j\}$ such that $\sum_j \vec{m}_j$ is on the plane p_n. Let m_j index the plane that contains $\vec{m}_j$, counting from the tip of the cone. Then this condition is equivalent to

$$\sum_j m_j = n. \tag{3.1}$$

Let us denote the number of integer coordinate points on the plane p_m by a_m. Then the problem is equivalent to the problem of partitioning an integer n in integer components m_j, with the added complication that at level m there are a_m inequivalent summands. This is a standard partition problem and the asymptotics is studied by Meinardus [12]; his theorem states that asymptotically the number of such partitions is given by

$$S(n) \equiv \log\{\# \text{ partitions of } n\} = \frac{\alpha+1}{\alpha}\left(An^\alpha \Gamma(\alpha+1)\zeta(\alpha+1)\right)^{\frac{1}{\alpha+1}} + \mathcal{O}(\log n). \tag{3.2}$$

Here A is the residue at the rightmost pole, located at $s = \alpha$, of the Dirichlet series $D(s)$ given by

$$D(s) \equiv \sum_{m=1}^{\infty} \frac{a_m}{m^s}. \tag{3.3}$$

Therefore, to find the multiplicities we need to know the coefficients a_m, i.e., the number of (integer coordinate) points on plane p_m. In the plethystic program, the integer a_m corresponds to the number of single-trace operators at level (distance) m, and the multiplicities we are after are integers d_j such that

$$\prod_{m=1}^{\infty} (1 - t^m)^{-a_m} = \sum_{j=0}^{\infty} d_j t^j. \tag{3.4}$$

Here the exponents of t parameterize the distance of a plane parallel to p from the tip of the dual cone. The quantities d_j are the numbers of multi-trace operators composed of the single trace ones. We will revisit this in Section 4.

Example: Let us see how this works for the two dimensional case portrayed in Figure 5, where we have chosen the lines (planes) to have slope -2 and the numbers a_m are given by $a_m = 1, 1, 2, 2, 3, \ldots \rightarrow 1 + [m/2]$. We see that indeed, $a_0, a_1, a_2, \ldots$ correspond to the
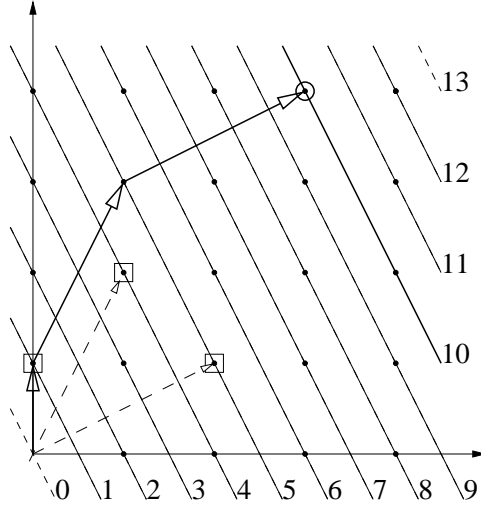
12

Figure 5: A two-dimensional partition example with one possible family of parallel lines with slope -2. The dark lattice points are the coordinate points and the numbers label the lines: p_n means the n-th line with slope -2 away from the origin. We have specifically chosen to draw the line p_{10} as a solid line while other lines p_m are dotted and for p_{10}, we have portrayed one possible partition of vectors summing up to the lattice points on it.

number of points on the lines $p_0, p_1, p_2, \ldots$ Clearly, for a general slope[3] $(-a)$ the coefficients are given by

$$a_m = 1 + \left[\frac{m}{a}\right] \stackrel{m \gg 1}{\approx} \frac{m}{a} + \mathcal{O}(1), \tag{3.5}$$

where $[x]$ denotes the integer part of x.

Plugging a_m into (3.3), we can evaluate the Dirichlet series to give

$$D(s) = \frac{1}{a}\zeta(s-1) + \cdots, \tag{3.6}$$

from which we find the location of the rightmost pole at $s = 2$, with residue $1/a$, i.e., $\alpha = 2$ and $A = 1/a$. The omitted terms give additional poles which are further to the left. Thus the Meinardus theorem yields

$$S(p_n) = \frac{3}{2}\left(\frac{n^2}{a}\Gamma(3)\,\zeta(3)\right)^{\frac{1}{3}} + \mathcal{O}(\log n). \tag{3.7}$$

Note that the quantity $An^\alpha = n^2/a$ in the Meinardus theorem is equal to twice the area of the triangle cut off from the cone by the p_n line. This will be true also in the three dimensional case: the coefficient An^α will be proportional to the volume of the pyramid cut off from the cone by the plane p_n. This will be of critical importance later; it allows us to sidestep intractable analytic computations via an elegant geometric construction.

---

[3] We assume $a > 1$; the opposite case clearly works similarly.

3.1.1 Explicit enumeration of the planar partitions

Let us now generalize from the two-dimensional example to a d-dimensional toric variety. For us the interesting dimension is $d = 3$, but working in a general dimension comes at no additional cost.

We start with the coefficients a_m: the number of integral points of the dual toric cone contained in the plane p_m. For large m, the number of integral points can be approximated by the $(d-1)$-dimensional area of the plane p_m. By dimensional arguments, this area scales as $a_m = \mathcal{A}m^{d-1}$, where $\mathcal{A}$ is a constant specified by the orientation of the plane in the cone. This allows us to evaluate the Dirichlet series (3.3) as

$$D(s) = \sum_{m=1}^{\infty} \frac{\mathcal{A}\,m^{d-1}}{m^s} + \text{corrections} = \mathcal{A}\,\zeta(s+1-d) + \text{corrections}\,. \tag{3.8}$$

This has the rightmost pole at $s = d$, with residue $\mathcal{A}$, yielding the parameters $\alpha = d$ and $A = \mathcal{A}$.

To evaluate $\mathcal{A}$, consider the number of integral points inside the pyramid cut off from the dual toric cone by the plane p_m. This can be approximated by the volume V_m of the pyramid. Again by dimensional arguments, for a d-dimensional cone this volume scales as $V_m = \lambda m^d$ for some λ. Clearly the number of points in the plane p_m can then be written as

$$a_m = V_m - V_{m-1} = \lambda(m^d - (m-1)^d) \approx \lambda d m^{d-1} + \mathcal{O}(m^{d-2}) \approx \frac{dV_m}{m}\,, \tag{3.9}$$

from which we find the residue

$$\mathcal{A} \equiv \frac{a_m}{m^{d-1}} \approx \frac{dV_m}{m^d}\,. \tag{3.10}$$

Using these results we can plug into (3.2) and write the number of partitions of vectors on plane p as

$$S(p) \equiv \ln(\#\text{ partitions}) = \frac{d+1}{d}\Big(V d\,\Gamma(d+1)\,\zeta(d+1)\Big)^{\frac{1}{d+1}} + \mathcal{O}(\log V)\,, \tag{3.11}$$

where V is the volume of the pyramid cut off from the cone by the plane p. We have dropped the index n in p_n because it is a function only of the particular plane in question, and not the additional family of auxiliary planes used in the construction.

We will need an explicit equation for the volume V later in Section 4 and will give the somewhat complicated expression there. For now we do not need such an explicit formula; it would even be a hindrance, as the analytic computations would quickly become hopelessly complicated, while simple geometric arguments can take us remarkably far.

3.2 Step 2: Partitions of individual vectors

Having found the partitions of all vectors lying on a given plane p, we now wish to use the results above to find the possible partitions of an individual vector $\vec{n}$. We shall accomplish

this by considering an upper bound on the number of such partitions, and then showing that asymptotically this bound is saturated.

Consider $\{p_{\vec{n},\vec{s}}\}$, the set of all planes containing the point $\vec{n}$. Here the subscript $\vec{s}$ indicates that the plane $p_{\vec{n},\vec{s}}$ is defined as being normal to $\vec{s}$, as well as containing $\vec{n}$. Note that for $p_{\vec{n},\vec{s}}$ to cut off a finite pyramid from the cone, we must have $(\vec{s},\vec{w}_a) > 0$ for all the edge generators $\vec{w}_a$ of the dual cone.[4] One can see that this condition is equivalent to $\vec{s}$ living inside the toric cone.[5] Continuing the above notation, we denote the volume of the pyramid cut out by the plane $p_{\vec{n},\vec{s}}$ as $V_{\vec{n},\vec{s}}$.

Since the point $\vec{n}$ is merely a point in the plane $p_{\vec{n},\vec{s}}$, the multiplicity of $\vec{n}$ is bounded by the multiplicity of $p_{\vec{n},\vec{s}}$. This gives:

$$e^{S(\vec{n})} \leq e^{S(p_{\vec{n},\vec{s}})} = \exp\left(\frac{d+1}{d}\left(d\,V_{\vec{n},\vec{s}}\Gamma(d+1)\zeta(d+1)\right)^{\frac{1}{d+1}}\right). \tag{3.12}$$

Since this is true for any plane $p_{\vec{n},\vec{s}}$, we can take a minimum over all the possible $\vec{s}$ on the right hand side of (3.12). This minimum is well defined because $\vec{s}$ lives inside the toric cone, and on the faces of the cone $V_{\vec{n},\vec{s}}$ diverges.[6] Thus a minimum will exist inside the cone. Defining the function $f(\vec{n})$ as

$$f(\vec{n}) = d \min_{\vec{s}} V_{\vec{n},\vec{s}}, \tag{3.13}$$

we can write (3.12) as

$$e^{S(\vec{n})} \leq \exp\left(\frac{d+1}{d}\left(f(\vec{n})\Gamma(d+1)\zeta(d+1)\right)^{\frac{1}{d+1}}\right). \tag{3.14}$$

Now we wish to argue that in an asymptotic limit this bound becomes saturated, and therefore (3.14) gives us the multiplicity we are after.

It is straightforward to see which $\vec{s}$ minimizes the expression (3.13): by construction the volume minimizing plane, $p_{\vec{n},\vec{s}_{min}}$, has to be tangent to surfaces of constant f, and therefore[7]

$$\vec{s}_{min} = \vec{\nabla}f(\vec{n}), \quad \text{so that } f(\vec{n}) = dV_{\vec{n},\vec{\nabla}f(\vec{n})}. \tag{3.15}$$

Thus, to any point $\vec{n}$ we can associate the volume minimizing plane

$$p(\vec{n}) \equiv p_{\vec{n},\vec{s}_{min}}. \tag{3.16}$$

In Sec. 3.3.1 below we show that $\vec{n}$ is the center of gravity of the polygon $p(\vec{n}) \cap \mathcal{C}^*$. The uniqueness of the center of gravity then establishes that $p(\vec{n})$ is injective. But this implies

---

[4] Since $\vec{s}$ and $-\vec{s}$ define the same plane, $(\vec{s},\vec{w}_a) < 0$ would work just as well. We choose > 0 without loss of generality.

[5] Note: not the dual cone $\mathcal{C}^*$, but the toric cone $\mathcal{C}$.

[6] This is because for $\vec{s} \in \partial\mathcal{C}$, the constraining planes become parallel to faces of $\mathcal{C}^*$. Thus, they fail to contain finite volumes within $\mathcal{C}^*$ so $V_{\vec{n},\vec{s}}$ diverges.

[7] To be precise, this argument only implies that $\vec{s}_{min}$ is proportional to the gradient $\vec{\nabla}f$, but since the normalization of $\vec{s}$ is immaterial, we can use this equation to fix the normalization.

that the point $\vec{n}$ maximizes the multiplicities on the plane $p(\vec{n})$. This is because, by the injectivity of the map p, all other points $\vec{n}'$ on the plane $p(\vec{n})$ must have different minimizing planes $p(\vec{n}')$ for which $\vec{n}'$ will be the center of gravity. Then, necessarily, $V_{p(\vec{n}')} < V_{p(\vec{n})}$, since $p(\vec{n}')$ is volume-minimizing plane for $\vec{n}'$. Thus,

$$e^{S(\vec{n}')} \leq e^{S(p(\vec{n}'))} < e^{S(p(\vec{n}))} = \exp\left(\frac{d+1}{d}\left(f(\vec{n})\Gamma(d+1)\zeta(d+1)\right)^{\frac{1}{d+1}}\right). \tag{3.17}$$

This then implies that

$$\frac{e^{S(p(\vec{n}))}}{A(p(\vec{n}))} \leq e^{S(\vec{n})} \leq e^{S(p(\vec{n}))} \tag{3.18}$$

where $A(p(\vec{n}))$ is the area of the volume minimizing plane passing through $\vec{n}$. The left hand inequality simply uses the fact that $S(\vec{n}) > S(\vec{n}')$ on the plane $p(\vec{n})$ while $e^{S(p(\vec{n}))} = \sum_{\vec{n}'} e^{S(\vec{n}')}$. The right hand inequality is (3.14). Now observe that the $A(p(\vec{n}))$ scales as $|\vec{n}|^{d-1}$ where we are taking the Euclidean norm. Thus, taking logarithms of both sides of (3.18) we get

$$S(p(\vec{n})) - \mathcal{O}(\log(|\vec{n}|)) \leq S(\vec{n}) \leq S(p(\vec{n})) \tag{3.19}$$

Now from (3.11) $S(p(\vec{n}))$ scales as $V^{\frac{1}{d+1}} \sim |\vec{n}|^{\frac{d}{d+1}}$. Thus we see that when $|\vec{n}|$ is large,

$$e^{S(\vec{n})} \approx e^{S(p(\vec{n}))} = \exp\left(\frac{d+1}{d}\left(f(\vec{n})\Gamma(d+1)\zeta(d+1)\right)^{\frac{1}{d+1}}\right), \quad \text{or}$$

$$S(\vec{n}) \approx \frac{d+1}{d}\left(f(\vec{n})\Gamma(d+1)\zeta(d+1)\right)^{\frac{1}{d+1}}. \tag{3.20}$$

This is the main result of this section. We have only kept leading terms in all expressions; to accurately evaluate multiplicities near the boundaries of $\mathcal{C}^*$ subleading terms will have to be kept too. Eq. (3.20) can be used to compute the number of multi-trace operators corresponding to any given triplet of charges, and thus gives a prediction for the entropy of the dual black holes on the gravity side.

Z-minimization revisited: Recall from Sec. 2.3.1 that the Reeb vector $\vec{b} = (b_1, b_2, 3)$ is computed by minimizing Z, which is proportional to the volume cut from $\mathcal{C}^*$ with a plane of the form $2(\vec{b}, \vec{n}) = 1$ [4]. Notice that all such planes pass through the point $\vec{n} = (0, 0, \frac{1}{6})$. The Reeb vector is therefore precisely the normal to the plane $p((0, 0, \frac{1}{6}))$ and indeed to all planes $p(0, 0, z)$:

$$\vec{b} \propto \vec{\nabla} f((0, 0, z)), \tag{3.21}$$

where the proportionality is set by requiring that $b_3 = 3$. The argument above eq. (3.17) then establishes that every point on the z-axis is the maximal entropy point on its own equal R-charge surface. Because these surfaces take the form

$$(\vec{b}, \vec{n}) = b_1 x + b_2 y + 3z = \frac{3R}{2}, \tag{3.22}$$
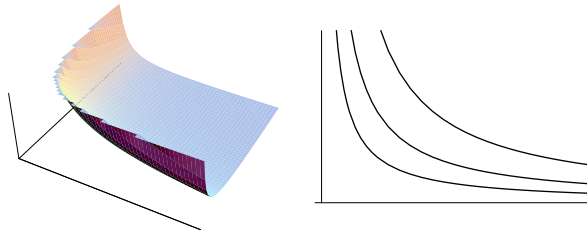
16

Figure 6: Equal entropy surfaces in the dual toric cone of $\mathbb{C}^3$. They take the form of generalized hyperboloids (in the interior of the cone; see left) and hyperbolae (on the faces of the cone; see right.) The interior surfaces represent parametrically higher entropies.

the point of maximal entropy of an equal R-charge surface is always given by

$$\left(0, 0, \frac{R}{2}\right). \tag{3.23}$$

In the next subsection we generalize this to arbitrary constraint surfaces. The result (3.23) holds in the standard presentation of the dual toric cone, that is when the Newton polygon lives in the plane $z = 1$.

Surfaces of constant entropy: From (3.20) we see that the surfaces of constant entropy in the dual toric cone are given by level sets of the function $f(\vec{n})$. From the definition of $f(\vec{n})$, these surfaces are characterized by the property that at each point $\vec{n}$ on the surface, the plane tangent to the surface at $\vec{n}$ cuts out an equal volume from the cone. Surfaces with this property are generalized hyperboloids in the cone. In Figure 6 we plot these surfaces of constant entropy.

It is also interesting to consider entropy on the faces of the cone. Although the preceding construction appears to assign zero entropy to these faces, this should taken as a statement that the entropy on the faces is parametrically smaller than inside the cone. A good example here is $\mathbb{C}^3$, where the interior of the cone corresponds to the $\frac{1}{8}$-BPS sector, i.e., operators composed of three fields {X,Y,Z}, while on the faces only two fields (say {X,Y}) are available. Evidently the entropy on the faces is parametrically lower but non-zero. The equal entropy curves on the faces take the form of hyperbolae. (See Figure 6.)

3.3 Maximizing entropy

In Section 3.2 we saw that the degeneracy of multi-trace operators with a specified d-tuple of charges $\vec{n}$ is entirely determined by the behavior of one function, $f(\vec{n})$, which was essentially given by the minimal volume that can be cut out from the dual toric cone with a $(d-1)$-plane containing $\vec{n}$. The normal to this minimizing plane is then given by the gradient $\vec{\nabla} f(\vec{n})$, and it is very useful to think of $\vec{\nabla} f(\vec{n})$ as the direction of the most rapid growth of entropy, starting from the point $\vec{n}$.

A problem of interest is to maximize entropy subject to a specified constraint, such as a fixed R-charge R. In the following we consider constraints which are linear in the charge vector $\vec{n}$. Such constraints trace $(d-1)$-hyperplanes in d-dimensions and take the form

$$c_{\vec{s}}(\vec{n}) = (\vec{s}, \vec{n}) - n_s = 0, \tag{3.24}$$

where $\vec{s}$ is the normal of the constraint plane, and n_s is proportional to the corresponding charge, with the proportionality constraint set by the normalization of $\vec{s}$. For the special case of fixed R charge, the normal to the constraint planes is given by the Reeb vector $\vec{b}$ of the toric variety, and the constraint equation reads $(\vec{b}, \vec{n}) - \frac{3}{2}R = 0$.

Maximizing entropy given a constraint $c_{\vec{s}}(\vec{n}) = 0$ is then accomplished using the standard Lagrange multiplier technique: the maximum is given by the point where the constraint plane is tangent to a surface of constant $f(\vec{n})$ which is equivalent to

$$\vec{\nabla} f(\vec{n}) \propto \vec{\nabla} c_{\vec{s}}(\vec{n}) = \vec{s}. \tag{3.25}$$

Unfortunately, due to the complicated analytic expression for the volume of a pyramid cut from the cone, equation (3.25) is difficult to work with analytically. Luckily, a simple geometric observation reduces this problem to a very tractable one, familiar from freshman mechanics.

3.3.1 Maximal entropy points as centers of gravity

We shall now show that the point of maximal multiplicity on a given plane is given by the center of gravity of that plane. This provides a simple prescription for finding the maximal entropy given an arbitrary constraint. Using the AdS/CFT correspondence, this will give the maximal entropy of a black hole in AdS space with charges satisfying the constraint. In particular, this will allow us to find the entropy and flavor charges of the most entropic black hole with R charge R.

Consider a linear constraint $c_{\vec{s}}(\vec{n}) = 0$, and denote the constraint plane by $p_{\vec{s}}$. Let the center of gravity of $p_{\vec{s}} \cap \mathcal{C}^*$ be $\vec{n}_0$. Now, pick an arbitrary line[8] l contained in the plane $p_{\vec{s}}$ that passes through the center of gravity $\vec{n}_0$. This is portrayed in Figure 7. To find the center of gravity, we define coordinates on the plane $p_{\vec{s}}$. We do so by choosing one of the coordinates, x, to be along l, and the other, y, to be perpendicular to l. Then the center of gravity is defined by the condition

$$\int_A dx\, dy\, y = 0\,, \tag{3.26}$$

where the integration is over the part of the plane $p_{\vec{s}}$ contained in the dual toric cone, i.e., $A = p_{\vec{s}} \cap \mathcal{C}^*$.

---

[8] For clarity, we present this argument for the three-dimensional cone. However, the same logic will go go through in an arbitrary dimension d.
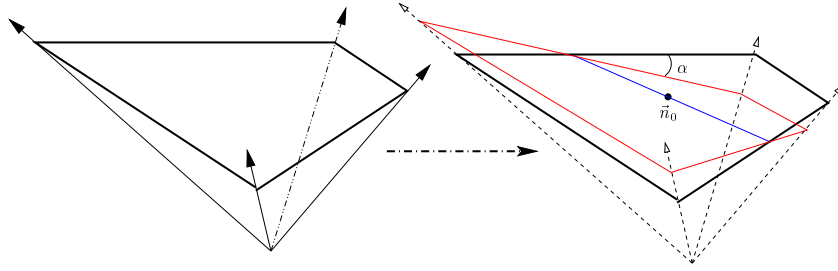
Figure 7: Left: A constraint plane slicing the dual toric cone. Right: A line l (in blue) through the center of gravity of the slice. The contour in red illustrates the change in the volume cut by the plane after it is tilted about l by the angle α. The toric variety used in the present example is the cone over dP_1.

Now, consider tilting the plane $p_{\vec{s}}$ around the axis l by a small angle α, as illustrated in Figure (7). Denoting this tilted plane by $p'_{\vec{s}}$, the change in volume cut from the cone can be written as

$$\Delta V = \int_{A'} dx\, dy\, y \sin \alpha \approx \alpha \int_A dx\, dy\, y + \mathcal{O}(\alpha^2), \tag{3.27}$$

where A' is the intersection of the tilted plane $p'_{\vec{s}}$ and the dual cone $\mathcal{C}^*$. The approximation in the equation above requires a little bit of explanation, as one needs to take into account the change of region of integration from A' to A. However, it is easy to see that this change will contribute terms that are proportional to α, and combined with the $\sin \alpha$ factor these corrections only show up at order $\mathcal{O}(\alpha^2)$. The condition that $p_{\vec{s}}$ is the volume minimizing plane, $\Delta V = 0$, is therefore equivalent to setting the torque about the axis l to vanish as in (3.26).

However, since the line l is an arbitrary line passing through the center of gravity $\vec{n}_0$, the above argument is valid for any such line, and therefore for any tilt about $\vec{n}_0$. It follows that the constraint plane $p_{\vec{s}}$ is the volume minimizing plane for the center of gravity $\vec{n}_0$, and therefore, the arguments from Section 3.2 tell us that $\vec{n}_0$ must be the most entropic point on the plane $p_{\vec{s}}$.

As a side note, the preceding argument affords a new characterization of the Reeb vector. In particular, $\vec{b}$ is the normal to the unique family of parallel planes p_n such that the center of gravity of $p_n \cap \mathcal{C}^*$ is contained in the z-axis (x_d-axis in d dimensions).[9] This observation is applicable in the standard presentation of the toric fan of $\mathcal{M}$, where the Newton polygon is contained in the plane $z = 1$.

In some practical situations, finding the center of gravity of an infinitesimally thin slice $(\vec{s}, \vec{n}) = c$ of the dual toric cone may still be harder than solving another auxiliary problem. Consider a family of parallel slices (constraints) of the form $(\vec{s}, \vec{n}) = c_i$, indexed by i. Because $\mathcal{C}^*$ is a cone, all such slices are similar polygons, differing only by an overall scale. This

---

[9] With a slight abuse of notation, we use z to denote a coordinate both on the toric cone and the dual toric cone.
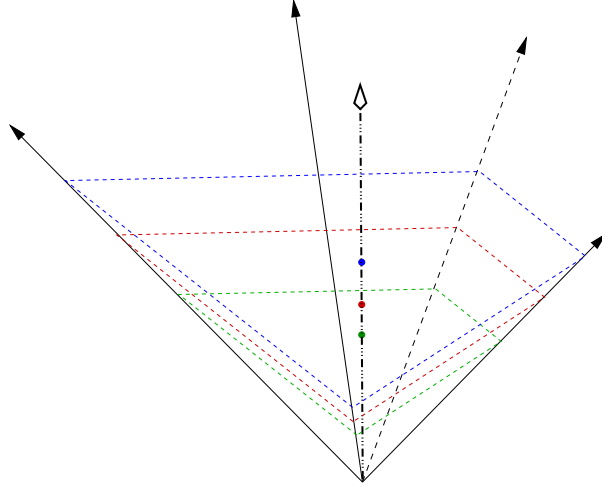
Figure 8: A family of parallel planar constraints intersecting the dual toric cone. All constraint slices are similar polygons, so their centers of gravity fall on a ray extending from the tip of the dual toric cone. Here the toric variety is dP_1. The constraint slices are normal to the Reeb vector and represent equal R surfaces. The diagram was drawn in the standard $SL(3, \mathbb{Z})$ frame, so that the centers of gravity of equal R-charge slices fall directly above the tip of the cone.

means that their centers of gravity all fall on the same straight line $k(\vec{s})$, which is uniquely determined by the normal vector $\vec{s}$ of the constraint plane. The intersection of this line with the constraint $(\vec{s}, \vec{n}) = c$ then yields the maximal degeneracy point on the plane. This is illustrated in Figure 8.

Now consider the pyramid $\Delta_{\vec{s}, c}$ cut out from the dual toric cone by the plane of constraint $(\vec{s}, \vec{n}) = c$. Its center of gravity also evidently lives on the line $k(\vec{s})$. We may now reverse the argument and find the line of maximal entropy, for this family of constraints given by $(\vec{s}, \vec{n}) = c_i$, by finding the center of gravity of the pyramid $\Delta_{\vec{s}, c}$. In particular, $k(\vec{s})$ is the ray extending from the tip of the cone in the direction of the center of gravity of $\Delta_{\vec{s}, c}$. In this way the point of maximum entropy on the constraint $(\vec{s}, \vec{n}) = c$ may be mechanistically recovered by hanging the pyramid by its tip using a piece of string. When the solid is balanced, the maximal entropy point will be directly below the tip.

The latter observation leads to a highly peculiar, mechanistic characterization of the Reeb vector. Consider the dual toric cone in standard presentation and align the z-axis (x_d-axis in d dimensions) with the vertical direction. Of all families of pyramids $\Delta_{\vec{s}, c}$, the family $\Delta_{\vec{b}, c}$ is the unique one whose centers of gravity will lie on the vertical axis, i.e., directly above the tip. In other words, if we chop the dual cone $\mathcal{C}^*$ with a plane normal to $\vec{b}$, the resulting pyramid will balance on its tip!
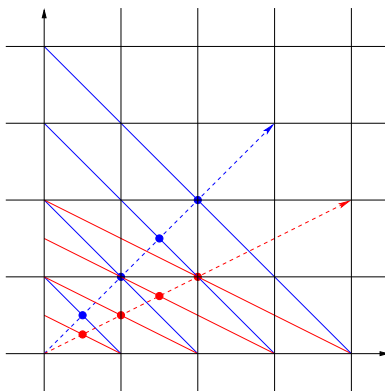
Figure 9: Two sets of constraints on the dual toric cone of $\mathbb{C}^2$. Level sets of the R-charge (normal to $\vec{b} = (1,1)$) and of the quantity $x + 2y = \frac{3}{2}R + y$ are given in blue and red, respectively. The midpoints of each set of line segments (bold dots) trace rays of fastest entropy growth for each set of constraints (dotted vectors).

3.3.2 Examples

We begin with the simplest possible example: $\mathbb{C}^2$ and take the dual toric cone to be the first quadrant of $\mathbb{Z}^2$, which is not the standard presentation. Here the Reeb vector is given by $\vec{b} = (1,1)$, and thus the lines corresponding to the constraint of fixed R charge are normal to $(1,1)$, i.e., they have slope -1. Here every equal R-charge constraint is a line segment normal to the Reeb vector $\vec{b} = (1,1)$. The center of gravity of each line segment is simply its midpoint, and the union of all midpoints forms the fastest growth ray $k(\vec{b}) = (1,1)$. This is drawn in blue in Fig. 9. The numeric equality between $\vec{b} = (1,1)$ and $k(\vec{b})$ is purely accidental[10] and is not respected by $SL(2, \mathbb{Z})$ transformations. One may wish to impose a different constraint, for example of the form $x + 2y = \text{const}$. The ray of maximal entropy is again given by the union of the midpoints of the line segments $x + 2y = c$ contained in the dual toric cone, and we can read off $k((1,2)) = (2,1)$. This is illustrated in red in Figure 9.

As a next example, consider the simplest three-dimensional toric variety. In its simplest presentation, where both the toric and the dual toric cone are simply the first octant of the lattice $\mathbb{Z}^3$, the symmetry relating the three generators is evident and trivially $k(\vec{b}) = (1,1,1)$. For a less trivial example, consider the presentation of the toric data of $\mathbb{C}^3$ in the conventions of Section 2, where we choose the $SL(3, \mathbb{Z})$ frame so that the generators of the toric cone reside in the $z = 1$ plane. It is straightforward to compute the generators of the dual toric cone and the Reeb vector using the results from Section 2, and one gets

$$w_1 = (0,1,0), \quad w_2 = (-1,-1,1), \quad w_3 = (1,0,0), \quad \vec{b} = (1,1,3). \tag{3.28}$$

Choosing the slicing corresponding to fixed R charge, i.e., the one corresponding to planes normal to the Reeb vector, we find that the center of gravity of the pyramid cut out from

---

[10] These two objects should not be compared, as $\vec{b} = (1,1)$ lives in the toric cone while $k(\vec{b})$ lives in the dual toric cone.

$\mathcal{C}^*$ by the plane of R-charge R, $x + y + 3z = \frac{3R}{2}$, is the point $(0, 0, \frac{3R}{8})$. Therefore the line of maximal entropy at fixed R-charge is given by

$$\vec{k}(\vec{b}) = \vec{k}((1, 1, 3)) = (0, 0, 1). \tag{3.29}$$

By the argument below eq. (3.21), this holds for every toric variety in the standard presentation. We remind the reader that $\vec{k}(\vec{s})$ is to be understood as specifying a ray, so its normalization is immaterial. The ray intersects the equal R surface at

$$(0, 0, \frac{R}{2}) = \frac{R}{2}(w_1 + w_2 + w_3), \tag{3.30}$$

in agreement with eq. (3.23). The form of (3.30), symmetric in the generators w_1, w_2, w_3, is a direct consequence of the fact that the three adjoint scalars X, Y, Z have equal R-charge. As exemplified here, all algorithms presented in the current section respect the $SL(3, \mathbb{Z})$ symmetry.

Finally, we treat the case of dP_1, which was used for illustration throughout Section 2. Again consider the family of equal R-charge constraints, which in the (standard) $SL(3, \mathbb{Z})$ frame of Figure 3 take the form

$$(4 - \sqrt{13})y + 3z = \frac{3}{2}R_0. \tag{3.31}$$

The center of gravity of the pyramid cut out from $\mathcal{C}^*$ with the plane (3.31) again resides at $(0, 0, \frac{3R_0}{8})$; indeed, this will hold for all pyramids formed by equal R-charge surfaces in the standard presentation. The most entropic charge vector for a fixed R-charge R_0 takes the form (3.23).

The appearance of an irrational number in the Reeb vector of dP_1, eq. (2.7), implies that an *exact* specification of the R-charge traces a line segment and not a plane intersecting $\mathcal{C}^*$. Namely, all the integer points in the dual toric cone that line within a plane perpendicular to the Reeb vector are actually collinear. In detail, writing down

$$R_0 = R_1 + R_2 \sqrt{13}, \tag{3.32}$$

the locus of equal R-charge takes the form

$$\begin{aligned} 4y + 3z &= \frac{3}{2}R_1 \\ -y &= \frac{3}{2}R_2, \end{aligned} \tag{3.33}$$

which is a line in three-space. However, such considerations would only be of practical import if one were capable of making *exact* R-charge (conformal dimension) measurements, so as to extract from one measurement two integers R_1, R_2. At any finite precision ϵ, the relevant constraint to impose instead is

$$R_0 - \epsilon < R < R_0 + \epsilon. \tag{3.34}$$

In this case, the most entropic point is given by the center of mass of the thin shell (3.34) and is given by (3.23). For completeness, we present in Appendix A an algorithm for calculating the multiplicity of operators matching a specified irrational R-charge *exactly* (analogously to eq. (3.11)). This generalizes the construction of Sec. 3.1.

3.4 Dual giant interpretation

Recalling the construction [4] reviewed in Sec. 2.4, wherein $\mathcal{C}^*$ is seen as the phase space of a dual giant graviton propagating in the $\text{AdS}_5 \times X$ background, one can also interpret the present results in terms of dual giant configurations. Dual giant gravitons are point-like objects from the viewpoint of the Sasaki-Einstein manifold X and carry momentum $\vec{P} = (P_{\phi_1}, P_{\phi_2}, P_{\phi_3})$ along the directions of the maximal torus of X. This momentum is quantized and takes integer values falling in the dual toric cone $\mathcal{C}^*$. In this way, the conserved momentum of each dual giant graviton $\vec{P}$ corresponds to a charge vector $\vec{m}$ comprising the three $U(1)$ (flavor) charges studied above. Likewise, we may think of a vector $\vec{s} \in \mathcal{C}$ as specifying a particular cycle $\sigma_{\vec{s}}$ in the maximal torus, and a planar surface

$$(\vec{s}, \vec{P}) = P_{\vec{s}} \tag{3.35}$$

consists of all states whose component of momentum along $\sigma_{\vec{s}}$ is fixed at $P_{\vec{s}}$. The result of Sec. 3.1, eq. (3.11), gives the total number of such configurations.

Analogously, Sec. 3.2 gives a way of enumerating the configurations of many dual giants which are characterized by a given triple of total momenta $\vec{P} = (P_{\phi_1}, P_{\phi_2}, P_{\phi_3})$. Following the procedure, eq. (3.15) assigns to $\vec{P}$ a special cycle corresponding to $\vec{\nabla} f(\vec{P}) \in \mathcal{C}$. Eq. (3.20) then shows that fixing the total momentum along that cycle becomes in the asymptotic regime equivalent to fixing the momentum vector at $\vec{P}$. The reason for that is reminiscent of the equipartition theorem and may be traced directly to the central limit theorem. In particular, the orientation of the cycle $\sigma_{\vec{\nabla} f(\vec{P})}$ in the maximal torus of X is such that momentum running along it splits among the fundamental cycles of the torus precisely in the ratio given by $\vec{P}$.

4 Universal distribution of trace factors

In the previous section we found the multiplicity of operators for any given triple of charges $\vec{n}$, comprising (linear combinations of) the R-charge and the two flavor charges. Further, we gave an algorithm which selects the combination of flavor charges $\vec{n}$ that maximizes this multiplicity given any linear constraint on the charges. In this section we will show that when $|\vec{n}|$ is large, most of these operators share a universal trace structure.

In [13], the structure of multi-trace operators in the half-BPS sector of $\mathcal{N} = 4$ SYM theory was treated using canonical partition function techniques. The problem of counting BPS multi-trace operators in an $\mathcal{N} = 1$ SCFT living on a finite stack of D-branes transverse

to the tip of a Calabi-Yau cone was likewise treated in [1] using the plethystic program. In the following we shall proceed along similar lines in order to extract statistical information about the distribution of traces in a multi-trace operator with charge vector $\vec{n}$.

As explained in Section 3, every multi-trace operator of charge vector $\vec{n}$ is specified by a vector partition

$$\sum_j \vec{m}_j = \vec{n}\,, \tag{4.1}$$

where each summand $\vec{m}_j \in \mathcal{C}^*$ corresponds to one trace factor, unique up to F-term relations. The exact correspondence between flavor charges, winding paths in the dimer model, and fields entering the given trace factor, was described in Section 2. Introducing a triple of generalized temperatures[11] $\vec{\beta} \equiv (\beta_1, \beta_2, \beta_3)$ and a chemical potential α , we may write down a grand canonical partition function for the system [1, 4]

$$Z = \prod_{\vec{m} \in \mathcal{C}^*} \left(1 - e^{\alpha - (\vec{\beta}, \vec{m})}\right)^{-1} \equiv \prod_{\vec{m} \in \mathcal{C}^*} Z_{\vec{m}}\,. \tag{4.2}$$

This partition function has been exhibited in [4] as counting dual giant graviton states moving on a toric variety $\mathcal{M}$, and concurrently in [1] as a generating function for mesonic multi-trace operators in the associated field theory. In the following, we first treat the case where $\alpha = 0$ so that every summand $\vec{m}$ (trace factor of type $\vec{m}$) is counted with the same weight. Indeed, each factor $Z_{\vec{m}} = \left(1 - e^{-(\vec{\beta}, \vec{m})}\right)^{-1}$ allows for an arbitrary number of repetitions of the summand $\vec{m}$ in a partition (multi-trace operator). Thus, in setting $\alpha = 0$, we are going to let the ensemble choose its optimal number of trace factors M. The case where M is fixed by hand with a non-trivial chemical potential is treated later in the section.

4.1   Ensemble with unrestricted number of traces

With $\alpha = 0$, the partition function (4.2) blows up at $\vec{0} \in \mathcal{C}^*$. This corresponds to the onset of Bose-Einstein condensation at the trivial point. However, the tip of the cone corresponds to a trivial factor in the structure of a multi-trace operator, and as such should not be counted in the total number of factors in a multi-trace operator. Therefore, the correct partition function to be analyzed is:

$$Z = \prod_{\vec{m} \in \mathcal{C}^* \setminus \vec{0}} \left(1 - e^{-(\vec{\beta}, \vec{m})}\right)^{-1} \equiv \prod_{\vec{m} \in \mathcal{C}^* \setminus \vec{0}} Z_{\vec{m}}\,. \tag{4.3}$$

For a given charge vector $\vec{n}$, the Lagrange multipliers $\vec{\beta}$ are set by requiring:

$$\langle n_i \rangle = -\frac{\partial \log Z}{\partial \beta_i} \qquad i = 1, 2, 3\,. \tag{4.4}$$

---

[11] These temperatures are not physical. They are Lagrange multipliers introduced for ease of calculation.
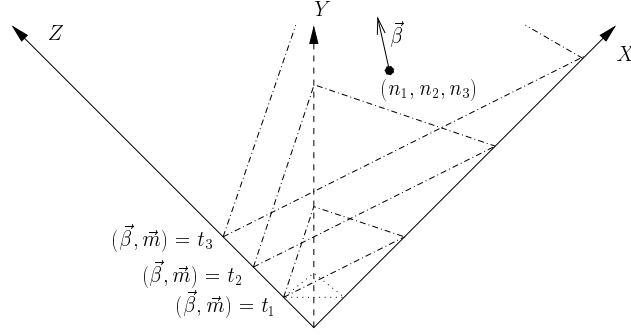
Figure 10: Illustration of the natural grading associated to the point (n_1, n_2, n_3) for $\mathbb{C}^3$. The planes with dashed lines are normal to $\vec{\beta}$, and for comparison we have included the level 1 surface containing $\operatorname{Tr} X$, $\operatorname{Tr} Y$ and $\operatorname{Tr} Z$ with dotted lines.

Because eq. (4.3) factorizes, we can read off the mean and standard deviation in the population of the trace factor $\vec{m}$:

$$\langle n_{\vec{m}} \rangle = -\frac{1}{m_i} \frac{\partial \log Z_{\vec{m}}}{\partial \beta_i} = (e^{(\vec{\beta}, \vec{m})} - 1)^{-1}. \tag{4.5}$$

The right hand side is manifestly independent of i. Indeed, (4.4) counts average charge while (4.5) counts the average number of traces; their relation is

$$\langle n_i \rangle = \sum_{\vec{m} \in \mathcal{C}^* \setminus \vec{0}} m_i \langle n_{\vec{m}} \rangle . \tag{4.6}$$

The standard deviation in $n_{\vec{m}}$ reads:

$$\sigma(n_{\vec{m}}) = \left(\langle n_{\vec{m}}^2 \rangle - \langle n_{\vec{m}} \rangle^2 \right)^{1/2} = \left(\frac{1}{m_i^2 Z_{\vec{m}}} \frac{\partial^2 Z_{\vec{m}}}{\partial \beta_i^2} - \left(e^{(\vec{\beta}, \vec{m})} - 1 \right)^{-2} \right)^{1/2} = \left(2 \sinh \frac{(\vec{\beta}, \vec{m})}{2} \right)^{-1}, \tag{4.7}$$

so that the standard deviation always exceeds the mean, most rampantly away from the tip of the cone:

$$\sigma(n_{\vec{m}}) / \langle n_{\vec{m}} \rangle = e^{\frac{(\vec{\beta}, \vec{m})}{2}} = \left(1 + \langle n_{\vec{m}} \rangle^{-1} \right)^{1/2} \geq 1 . \tag{4.8}$$

This is the same relation as that found in [13]. We defer a full discussion of the structure of heavy multi-trace operators until the next subsection.

Eq. (4.5) shows that the planar surfaces

$$(\vec{\beta}, \vec{m}) = y \tag{4.9}$$

share the same occupation numbers. This induces a natural grading of the dual cone $\mathcal{C}^*$ by parallel planes with the normal $\vec{\beta}$; we illustrate this in Figure 10. It is easy to see that these planes are the same as the planes p_m utilized in Sections 3.1, 3.2 to evaluate the number

of vector partitions of a given vector $\vec{n}$.[12] Consequently $\vec{\beta} \parallel \vec{\nabla} f(\vec{n})$ and we may recast the populations at sites $\vec{m}$ in terms of just one temperature β:

$$\langle n_{\vec{m}} \rangle = -\frac{1}{(\vec{m}, \vec{\nabla} f(\vec{n}))} \frac{\partial \log Z_{\vec{m}}}{\partial \beta} = (e^{\beta (\vec{m}, \vec{\nabla} f(\vec{n}))} - 1)^{-1}, \qquad (4.10)$$

where we have set

$$\vec{\beta} \equiv \beta \vec{\nabla} f(\vec{n}). \qquad (4.11)$$

With this form of $\vec{\beta}$ substituted in eq. (4.3), the condition setting β reads:

$$(\vec{n}, \vec{\nabla} f(\vec{n})) = -\frac{\partial \log Z}{\partial \beta}. \qquad (4.12)$$

For large $|\vec{n}|$, we can use a continuum approximation. A thin shell contained between two planes normal to $\vec{\nabla} f(\vec{n})$ given by

$$t < (\vec{m}, \vec{\nabla} f(\vec{n})) < t + dt \qquad (4.13)$$

is seen from eq. (3.9) to contain

$$a_t \, dt = \frac{V_t \, d}{t} dt \qquad (4.14)$$

lattice points. In order to write an explicit expression for V_t in d dimensions, we shall need further notation. Write the dual toric cone $\mathcal{C}^*$ as a union of F simplicial cones $\hat{\sigma}^i$ and denote the d generators of $\hat{\sigma}^i$ by $\hat{\vec{w}}^i_j$, $j = 1, \ldots, d$. Each of these is a d-vector, so $(\hat{w}^i)_{jk}$ is a $d \times d$ matrix. In terms of the notation of Sec. 2.3, which is suitable to $d = 3$, one choice of the F simplicial cones leads to:

$$\begin{aligned}
\hat{\vec{w}}^i_1 &= \vec{w}_{k-1,0} \\
\hat{\vec{w}}^i_2 &= \vec{w}_{i-1,i} \\
\hat{\vec{w}}^i_3 &= \vec{w}_{i,i+1}
\end{aligned} \qquad (4.15)$$

Here i ranges from 0 to $F = k - 2$, where the Newton polygon is a k-gon. The volume of the dual toric cone bound by the plane $(\vec{s}, \vec{x}) = t$ with normal $\vec{s}$ is then given by

$$V_t = \frac{t^d}{d!} \sum_{i=1}^{F} \frac{|\det \hat{w}^i|}{\prod_{j=1}^{d} (\hat{\vec{w}}^i_j, \vec{s})}. \qquad (4.16)$$

It follows that the thin shell (4.13) contains

$$\frac{1}{(d-1)!} \sum_{i=1}^{F} \frac{|\det \hat{w}^i|}{\prod_{j=1}^{d} (\hat{\vec{w}}^i_j, \vec{\nabla} f(\vec{n}))} t^{d-1} dt \equiv B(\vec{n}) \, t^{d-1} dt \qquad (4.17)$$

---

[12] This follows from the observation that the counting procedure in Sections 3.1, 3.2 did not distinguish among charge vectors lying on the same plane p_m. Thus, the planes p_m comprise vectors of equal multiplicity, as do the planes (4.9), so the two families must coincide.

lattice points. Recalling from the definition (3.15) that $f(\vec{n}) = V_t\, d$ for $t = (\vec{n}, \vec{\nabla} f(\vec{n}))$, we see that $B(\vec{n})$ may be related to $f(\vec{n})$ as

$$B(\vec{n}) = \frac{V_t\, d}{t^d} = \frac{f(\vec{n})}{(\vec{n}, \vec{\nabla} f(\vec{n}))^d} \ , \tag{4.18}$$

that is,

$$f(\vec{n}) = (\vec{n}, \vec{\nabla} f(\vec{n}))^d\, B(\vec{n}) = \frac{(\vec{n}, \vec{\nabla} f(\vec{n}))^d}{(d-1)!} \sum_{i=1}^{F} \frac{|\det \hat{w}_i|}{\prod_{j=1}^{d} (\hat{\vec{w}}_{ij}, \vec{\nabla} f(\vec{n}))} \ . \tag{4.19}$$

Now, each of the points in the thin shell has mean population $(\exp \beta\, t - 1)^{-1}$, and contributes t to the right hand side of eq. (4.12), as a continuous version of (4.6). Therefore, we may approximate the condition (4.12) for β by an integral:

$$B(\vec{n}) \int_0^\infty \frac{t^d}{e^{\beta t} - 1}\, dt = (\vec{n}, \vec{\nabla} f(\vec{n})) \,, \tag{4.20}$$

where the negligible contribution for large t was added to the integral to facilitate explicit evaluation. Evaluating the integral, we get

$$\beta^{d+1} = \frac{B(\vec{n})\, \Gamma(d+1)\, \zeta(d+1)}{(\vec{n}, \vec{\nabla} f(\vec{n}))} \,, \tag{4.21}$$

which, using eqs. (3.20) and (4.19), yields an identity:

$$\beta = \frac{d}{d+1} \frac{S(\vec{n})}{(\vec{n}, \vec{\nabla} f(\vec{n}))} \tag{4.22}$$

Eq. (4.21) is in agreement with the well known case $d = 1$. There $f(n) = n$ so that $B(n) = 1$ and $\beta^2 = \zeta(2)/n$, as in eq. (3.7) of [14]. In the case of primary interest, $d = 3$, in the notation of Sec. 2.3, β takes the form:

$$\beta = \pi \left(\frac{1}{30\, (\vec{n}, \vec{\nabla} f(\vec{n}))\, (\vec{\nabla} f(\vec{n}), \vec{w}_{k-1,0})} \sum_{i=1}^{k-2} \frac{(\vec{w}_{k-1,0}, \vec{w}_{i-1,i}, \vec{w}_{i,i+1})}{(\vec{\nabla} f(\vec{n}), \vec{w}_{i-1,i})\, (\vec{\nabla} f(\vec{n}), \vec{w}_{i,i+1})} \right)^{1/4} \tag{4.23}$$

4.1.1 Structure of heavy multi-trace operators

Eqs. (4.10, 4.17, 4.21) allow us to uncover a wealth of information about the structure of a typical large charge multi-trace operator. We list such observations below.

The average number of trace factors in the operator is given by:

$$\langle M(\vec{n}) \rangle_0 = B(\vec{n}) \int_0^\infty \frac{t^{d-1}}{e^{\beta t} - 1}\, dt = \frac{B(\vec{n})\, \Gamma(d)\, \zeta(d)}{\beta^d} \tag{4.24}$$

27

Now, using the relation between $f(\vec{n})$ and $B(\vec{n})$ from (4.19), we therefore have

$$
\begin{aligned}
\langle M(\vec{n}) \rangle_0 &= \frac{B(\vec{n}) \, \Gamma(d) \, \zeta(d)}{(B(\vec{n}) \, \Gamma(d+1) \, \zeta(d+1))^{\frac{d}{d+1}}} (\vec{n}, \vec{\nabla} f(\vec{n}))^{\frac{d}{d+1}} \\
&= \frac{B(\vec{n}) \, \Gamma(d) \, \zeta(d)}{(B(\vec{n}) \, \Gamma(d+1) \, \zeta(d+1))^{\frac{d}{d+1}}} \left(\frac{f(\vec{n})}{B(\vec{n})} \right)^{\frac{1}{d+1}} \\
&= \frac{\zeta(d)}{d \, \zeta(d+1)} \Big(f(\vec{n}) \, \Gamma(d+1) \, \zeta(d+1) \Big)^{\frac{1}{d+1}} = \frac{\zeta(d)}{(d+1) \, \zeta(d+1)} \, S(\vec{n}) . \quad (4.25)
\end{aligned}
$$

In the first line we substituted for β^{-d} from eq. (4.21) and in the second for $(\vec{n}, \vec{\nabla} f(\vec{n}))$ from eq. (4.19). The average number of traces is directly proportional to the entropy, with the constant of proportionality determined solely by the dimension of the toric variety d.

The mean multiplicity $\langle n_{\vec{m}} \rangle$ of the $\vec{m}$-trace in the large multi-trace operator, eq. (4.10), quickly drops to 0 as $|\vec{m}|$ increases. The only traces whose occupations are of the order of 1 or greater are those satisfying

$$
\beta \, (\vec{m}, \vec{\nabla} f(\vec{n})) \lesssim \mathcal{O}(1) . \quad (4.26)
$$

By eq. (4.8), the same relation with a $\ll$ sign defines the regime where the mean *accurately* predicts a non-zero occupancy. Substituting for β from eqs. (4.21, 4.22), we have:

$$
\frac{(\vec{m}, \vec{\nabla} f(\vec{n}))}{(\vec{n}, \vec{\nabla} f(\vec{n}))} \lesssim \frac{d+1}{d \, S(\vec{n})} \iff (\vec{m}, \vec{\nabla} f(\vec{n})) \lesssim \left(\frac{(\vec{n}, \vec{\nabla} f(\vec{n}))}{\Gamma(d+1) \, \zeta(d+1) \, B(\vec{n})} \right)^{\frac{1}{d+1}} . \quad (4.27)
$$

This scaling behavior motivates the introduction of an auxiliary variable

$$
y(\vec{m}) \equiv \beta \, (\vec{m}, \vec{\nabla} f(\vec{n})) . \quad (4.28)
$$

In comparison with the variable t of eq. (4.13), y is rescaled by $y = \beta t$. It is clear that mean occupation numbers and all other quantities which are extractable from $Z(\beta)$ are functions of y alone. It is convenient to introduce the quantity

$$
x(y) = \int_0^y \frac{\tilde{y}^{d-1} d\tilde{y}}{e^{\tilde{y}} - 1} \Big/ \int_0^\infty \frac{\tilde{y}^{d-1} d\tilde{y}}{e^{\tilde{y}} - 1} . \quad (4.29)
$$

By the same logic which led to eqs. (4.20, 4.24), the quantity $x(y)$ gives that fraction of trace factors making up a heavy multi-trace operator (given by (4.24)) which have $\tilde{y} < y$. The graph of $x(y)$ is therefore a convenient presentation of *all the universal features* of a heavy multi-trace mesonic BPS operator. Importantly, $x(y)$ depends only on the dimension of the toric variety d, which motivates the notation $x_d(y)$. This leads to the interesting conclusion that in all world-volume SCFTs on D3-branes transverse to tips of toric Calabi-Yau threefolds, all heavy BPS operators are described by the same curve $x_3(y)$. The curves $x_2(y)$, $x_3(y)$, and $x_4(y)$ are plotted in Figure 11.
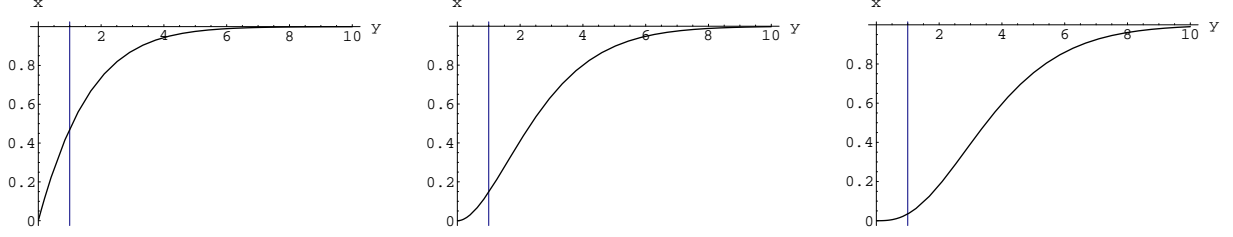
Figure 11: Left to right: $x_2(y)$, $x_3(y)$, $x_4(y)$.

The graphs $x_d(y)$ are interpreted as follows (we leave a speculative interpretation to Appendix C). Suppose one is interested in the structure of a heavy multi-trace mesonic BPS operator with charge vector $\vec{n}$. One begins by computing $B(\vec{n})$ from eq. (4.17) and β from eq. (4.21). The number of trace factors in equivalence classes $\vec{m}$ satisfying

$$\beta^{-1}y < (\vec{m}, \vec{\nabla}f(\vec{n})) < \beta^{-1}(y+dy) \tag{4.30}$$

is given by

$$\frac{B(\vec{n})}{\beta^d} \int_0^\infty \frac{\tilde{y}^{d-1}d\tilde{y}}{e^{\tilde{y}} - 1} \left(\frac{dx}{dy}\right) dy. \tag{4.31}$$

Here we have differentiated eq. (4.29) and used eq. (4.24) with $\tilde{y} = \beta t$. Using eq. (4.17) one may also evaluate the average number of trace factors corresponding to an individual site $\vec{m}$. This is given by

$$\langle n_{\vec{m}} \rangle = \langle n_{y(\vec{m})} \rangle = \frac{1}{y(\vec{m})^{d-1}} \left(\frac{dx}{dy}\right) \int_0^\infty \frac{\tilde{y}^{d-1}d\tilde{y}}{e^{\tilde{y}} - 1}. \tag{4.32}$$

Curiously, mean occupations per site depend only on the orientation of the vector $\vec{n}$ in $\mathcal{C}^*$.

Since the quantity $x_d(y)$ stands for the fraction of trace factors with $\tilde{y} < y$, it varies between 0 and 1. In particular, $1 - x(y)$ is the fraction of operators with $\tilde{y}$ exceeding y. From the fact that $x(y)$ approaches 1 very rapidly for y of the order of unity one sees that *almost all* summands satisfy $|\vec{m}| \propto |\vec{n}|^{\frac{1}{d+1}}$. The characteristic scale on which the occupations (4.32) vary is thereby set by the quantity $|\vec{n}|^{\frac{1}{d+1}}$.

Recalling eq. (4.26), the sites with occupations of the order of 1 or greater correspond to the section of the graph with $y < 1$. These are also the sites for which the mean occupancies (4.10, 4.32) are good predictors for actual occupation numbers. Since $x_3(1) \approx 0.15$, we see that approximately 85% of the trace factors entering a heavy operator are randomly selected from a large volume in $\mathcal{C}^*$. The size of that volume is such that $y > 1$ but still of the order of unity. In particular, $x_3(10) \approx 0.998$, which means that on average only 1 in 500 trace factors has $(\vec{m}, \vec{\nabla}f(\vec{n})) > 10\,(\vec{n}, \vec{\nabla}f(\vec{n}))^{\frac{1}{d+1}}$.

Denote the inverse of $x_d(y)$ as $y_d(x)$, so that $y_d(x_d(\tilde{y})) = \tilde{y}$. Consider the differential segment $(x, x + dx)$. It stands for $\langle M(\vec{n}) \rangle_0\, dx$ traces, each contributing $\beta^{-1}y_d(x)$ to the right hand side of eq. (4.20). Therefore, $y_d(x)\, dx$ is proportional to that fraction of the total

charge of the heavy operator, which is carried by the traces with $y_d(x) < \tilde{y} < y_d(x + dx)$. In particular, the charge carried by the trace operators with $\tilde{y}$ not exceeding y is given by

$$R'(\tilde{y} < y) \propto \int_0^{x_d(y)} \tilde{y}_d(x)\, dx \propto \int_0^y \tilde{y}\, \frac{\tilde{y}^{d-1}}{e^{\tilde{y}} - 1}\, d\tilde{y} \ \propto \ x_{d+1}(y)\,. \tag{4.33}$$

Here we performed a simple change of variable using the definition of $x_d(y)$, eq. (4.29). Eq. (4.33) holds for any charge of interest R' because for any linear combination of the d $U(1)$ charges the total charge grows proportionately as one includes factors of increasing y. In conclusion, the function $x_{d+1}(y)$ gives the fraction of the total charge of the operator residing in trace factors with $\tilde{y} < y$. As an example, $x_4(1) \approx 3\%$, which means that only 3% of the total charge of a heavy operator is carried by trace factors whose expected occupancies are of the order unity or greater. The remainder is contained in trace factors which are randomly pooled from the volume $(\vec{n}, \vec{\nabla} f(\vec{n}))^{\frac{1}{d+1}} < \beta^{-1} y < \kappa\, (\vec{m}, \vec{\nabla} f(\vec{n}))^{\frac{1}{d+1}}$, where $\kappa \gtrsim 1$.

4.2 Ensemble with a fixed number of traces

We now turn to the case where $\alpha < 0$. The condition (4.4) is supplemented by a condition fixing the number of traces M. In keeping with the standard language of the grand canonical ensemble, we shall alternately refer to trace factors as the *particles* of the system. The condition sets the parameter α:

$$M = \frac{\partial \log Z}{\partial \alpha}\,. \tag{4.34}$$

Here Z is again as given by equation (4.2) and includes $\vec{0} \in \mathcal{C}^*$. The results (4.5-4.8) are altered simply by substituting:

$$(\vec{\beta}, \vec{m}) \to (\vec{\beta}, \vec{m}) - \alpha \tag{4.35}$$

and as a consequence, the planar surfaces (4.9) continue to comprise points of equal occupations. One consequence of that is that the validity of Sec. 3.3.1 will also extend to the present section: on each plane p intersecting $\mathcal{C}^*$, the charge vector of maximal entropy *in the M-trace sector* is the center of gravity of $\{p \cap \mathcal{C}^*\}$. Furthermore, the argument which motivated (4.11) also continues to apply. Thus, we shall keep on referring to the scalar quantity β under the identification $\vec{\beta} \equiv \beta\, \vec{\nabla} f(\vec{n})$.

Proceeding as in Sec. 4.1, we approximate eqs. (4.4, 4.34) by integrals:

$$(\vec{n}, \vec{\nabla} f(\vec{n})) \ = \ B(\vec{n}) \int_0^\infty \frac{t^d dt}{e^{\beta t - \alpha} - 1} = \frac{B(\vec{n})\,\Gamma(d+1)\,g_{d+1}(e^\alpha)}{\beta^{d+1}} \tag{4.36}$$

$$M \ = \ B(\vec{n}) \int_0^\infty \frac{t^{d-1} dt}{e^{\beta t - \alpha} - 1} = \frac{B(\vec{n})\,\Gamma(d)\,g_d(e^\alpha)}{\beta^d}\,, \tag{4.37}$$

where $g_\nu(e^\alpha)$ stand for Bose-Einstein, or polylogarithm functions. We recall the definition to be $g_\nu(z) := \sum_{k=1}^\infty \frac{z^k}{k^n}$.

Using eq. (4.19) to eliminate β from the both equations, we get:

$$M = \frac{B(\vec{n})\,\Gamma(d)\,g_d(e^\alpha)}{\left(B(\vec{n})\,\Gamma(d+1)\,g_{d+1}(e^\alpha)\right)^{\frac{d}{d+1}}}\,(\vec{n},\,\vec{\nabla}f(\vec{n}))^{\frac{d}{d+1}} = \frac{\Gamma(d)\,g_d(e^\alpha)}{\left(\Gamma(d+1)\,g_{d+1}(e^\alpha)\right)^{\frac{d}{d+1}}}\,f(\vec{n})^{\frac{1}{d+1}}\,. \quad (4.38)$$

Eq. (4.38) allows one to set α independently of β. However, the coefficient of $f(\vec{n})^{\frac{1}{d+1}}$ in (4.38) is bounded from above by

$$\kappa(d) = \frac{\Gamma(d)\,\zeta(d)}{\left(\Gamma(d+1)\,\zeta(d+1)\right)^{\frac{d}{d+1}}} \quad (4.39)$$

since $0 \leq e^\alpha \leq 1$. For the case of most interest, $d = 3$, we have

$$\kappa(3) \approx 0.59\,. \quad (4.40)$$

This quantity marks the critical number of trace factors for the onset of Bose-Einstein condensation. Accordingly, we define

$$M_{\mathrm{crit}}(\vec{n}) = \kappa(d)\,f(\vec{n})^{\frac{1}{d+1}} \quad (4.41)$$

as the critical number of traces for a given charge vector $\vec{n}$. Note that in the $\alpha = 0$ case, wherein we let the ensemble choose its number of traces, we had

$$\langle M(\vec{n})\rangle_0 = M_{\mathrm{crit}}(\vec{n})\,, \quad (4.42)$$

as can be easily verified from eq. (4.25). For $M \neq M_{\mathrm{crit}}$, we distinguish the following cases:

4.2.1 The classical phase

For $M < M_{\mathrm{crit}}(\vec{n})$, $\langle n_{\vec{0}} \rangle$ is a finite number, so including or excluding the tip of the cone (contrast the products in eq. (4.2) and eq. (4.3)) is immaterial. In this case the condition (4.34) may equally well be taken to specify the *exact* number of traces or the *maximal* number of traces. We call this regime the classical phase, to distinguish it from the Bose-Einstein phase below. For completeness, we quote the usual formula for the entropy in the classical phase:

$$S(\vec{n}, M) = \log Z + \beta(\vec{n}, \vec{\nabla}f(\vec{n})) - \alpha M\,. \quad (4.43)$$

4.2.2 Bose-Einstein phase with trivial point included

When $M > M_{\mathrm{crit}}(\vec{n})$, a macroscopic proportion of trace factors condense on a small set of points and the system enters the Bose-Einstein phase. Depending on whether one works with partition function (4.2) or (4.3), that set of points is either the tip of the cone or the points nearest to it.

We begin by including the trivial point and consider partition function (4.2). This corresponds to fixing the *maximal* number of traces at M. The requisite counting is given

by the generating function $g_M(\vec{t})$ in [1]. In this case, the condensate at $\vec{0}$ corresponds to $M - M_{\mathrm{crit}}(\vec{n}) > 0$ excess trace factors, which the system dumps in the immaterial ground state. The physical meaning of the Bose-Einstein condensate is clear: it is the phase where it is more entropically favorable for the system to decrease the number of (non-trivial) trace factors.

Following the standard treatment of Bose-Einstein condensates, we have

$$(\vec{n}, \vec{\nabla}f(\vec{n})) = \frac{B(\vec{n})\,\Gamma(d+1)\,\zeta(d+1)}{\beta^{d+1}} \tag{4.44}$$

$$\alpha = -\frac{1}{M_{\mathrm{bc}}} + \mathcal{O}(M_{\mathrm{bc}}^{-2}), \tag{4.45}$$

where in the second line we assumed M_{bc}, the population of the condensate, to be large. The entropy takes the form:

$$\begin{aligned} S(\vec{n}, M) &= \log Z + \beta(\vec{n}, \vec{\nabla}f(\vec{n})) - \alpha(M - M_{\mathrm{bc}}) \\ &= \log Z + \beta(\vec{n}, \vec{\nabla}f(\vec{n})) + \frac{M_{\mathrm{crit}}(\vec{n})}{M_{\mathrm{bc}}} + \mathcal{O}(M_{\mathrm{bc}}^{-2}). \end{aligned} \tag{4.46}$$

In the large M_{bc} limit, only the first two terms remain. These, of course, correspond to the entropy contained in the $M_{\mathrm{crit}}(\vec{n})$ excited particles (non-trivial traces.) Therefore, (4.46) is expected to agree with (3.20) by the standard arguments establishing the equivalence of the microcanonical and grand canonical analyzes in the thermodynamic limit.

4.2.3 Bose-Einstein phase with trivial point excluded

We now work with the partition function

$$Z = \prod_{\vec{m} \in \mathcal{C}^* \backslash \vec{0}} \left(1 - e^{\alpha - (\vec{\beta}, \vec{m})}\right)^{-1} \equiv \prod_{\vec{m} \in \mathcal{C}^* \backslash \vec{0}} Z_{\vec{m}}. \tag{4.47}$$

This case corresponds to fixing the *exact* number of traces at $M > M_{\mathrm{crit}}(\vec{n})$.

Each state in the system is characterized by a choice of $n_{\vec{m}}$ such that

$$\sum_{\vec{m}} n_{\vec{m}}\,\vec{m} = \vec{n}. \tag{4.48}$$

As seen from eqs. (4.10, 4.35), the occupations $n_{\vec{m}}$ are controlled by the quantity $y(\vec{m}) = (\vec{m}, \vec{\nabla}f(\vec{n}))$, which plays the role of the energy of the system. With the tip of the cone excluded, the Bose-Einstein condensate will accumulate on those integral points in $\mathcal{C}^*$ for which $y(\vec{m})$ is the smallest. We denote this minimal value with y_0. The structure of a state as a vector partition (4.48) descends to a partition of the quantity $y(\vec{n}) = (\vec{n}, \vec{\nabla}f(\vec{n}))$:

$$y(\vec{n}) = \sum_{\vec{m}} n_{\vec{m}}\,y(\vec{m}) = M_{\mathrm{bc}}\,y_0 + \sum_{\vec{m} \notin \mathrm{bc}} n_{\vec{m}}\,y(\vec{m}). \tag{4.49}$$

32

In the last equality we have grouped the contributions to $y(\vec{n})$ of the Bose-Einstein condensate and of the excited particles, respectively.

Let $0 < c < 1$ be the proportion of $y(\vec{n})$ contributed by the second term in (4.49):

$$\sum_{\vec{m} \notin \mathrm{bc}} n_{\vec{m}} \, y(\vec{m}) \;=\; c \, y(\vec{n}) \qquad\qquad \Rightarrow \qquad\qquad \sum_{\vec{m} \notin \mathrm{bc}} n_{\vec{m}} \, \vec{m} = c \, \vec{n} \tag{4.50}$$

$$M_{\mathrm{bc}} \, y_0 \;=\; (1 - c) \, y(\vec{n}) \tag{4.51}$$

The condensate does not begin to set in until the population of all the excited particles reaches the critical value. The latter is given by

$$M_{\mathrm{crit}}(c\vec{n}) = c^{\frac{d}{d+1}} M_{\mathrm{crit}}(\vec{n}) \tag{4.52}$$

since the charge vectors of the excited particles form a partition of $c\vec{n}$ as in eq. (4.50). The scaling of $M_{\mathrm{crit}}(c\vec{n})$ with c follows from the definition (4.41) and the fact that $f(\vec{n})$ is a d-dimensional volume. Then imposing the condition that the total number of traces be M is equivalent to requiring:

$$M = (1 - c)\frac{y(\vec{n})}{y_0} + c^{\frac{d}{d+1}} M_{\mathrm{crit}}(\vec{n}) \,. \tag{4.53}$$

Using the fact that eq. (4.50) is a partition of $c\vec{n}$ with a critical number of traces, one may feed the solution of (4.53) into eq. (4.20) to get:

$$c\beta^{d+1} = \frac{B(\vec{n}) \, \Gamma(d + 1) \, \zeta(d + 1)}{(\vec{n}, \, \vec{\nabla} f(\vec{n}))} \,. \tag{4.54}$$

As before, the chemical potential in the large M_{bc} approximation is given by

$$\alpha \approx -\frac{1}{M_{\mathrm{bc}}} = -(1 - c)^{-1} \frac{y_0}{y(\vec{n})} \,. \tag{4.55}$$

This yields for the entropy

$$\begin{aligned} S(\vec{n}, M) &= \log Z + c \, \beta (\vec{n}, \, \vec{\nabla} f(\vec{n})) - \alpha (M - M_{\mathrm{bc}}) \\ &\approx \log Z + \frac{B(\vec{n}) \, \Gamma(d + 1) \, \zeta(d + 1)}{\beta^d} + \frac{c^{\frac{d}{d+1}}}{1 - c} \frac{y_0 M_{\mathrm{crit}}(\vec{n})}{y(\vec{n})} \,. \end{aligned} \tag{4.56}$$

At fixed $\vec{n}$, the limit of large M is the limit of small c and consequently, from eq. (4.54), large β. In the latter case, we see that every term in (4.56) goes to 0. This, of course, agrees with the intuition from the microcanonical counting: when the number of summands grows too large, the number of partitions of $\vec{n}$ quickly decreases, reaching 0 when $M \propto |\vec{n}|$.

4.3 Typical configurations of dual giant gravitons

As in Sec. 3, the results of the present section afford an interpretation in terms of dual giant graviton configurations. Indeed, the partition function (4.2) has been written down in [4] specifically to count configurations of dual giant gravitons. In particular, given the total momentum $\vec{P}$ on the maximal torus of X, a typical distribution of momenta of the individual dual giant gravitons is recovered using eq. (4.10) and its generalization as in eq. (4.35). This is done, as in Sec. 3, by selecting a special cycle $\sigma_{\vec{\beta}} \equiv \sigma_{\vec{\nabla} f(\vec{P})} \in \mathcal{C}$. One then sets the momentum component along $\sigma_{\vec{\nabla} f(\vec{P})}$ for each dual giant graviton using the (grand) canonical ensemble. The distribution of 3-momenta of the individual dual giant gravitons follows from this procedure for essentially statistical reasons: the cycle $\sigma_{\vec{\nabla} f(\vec{P})}$ is selected in such a way that momentum along it splits into the three fundamental cycles of the torus precisely in the ratio given by $\vec{P}$.

The different ensembles considered above have natural interpretations in the language of dual giant gravitons. For completeness, we dilate on this below:

1. The analysis of Sec. 4.1 applies to the case where one sets the total momentum of the dual giant gravitons to $\vec{P} \sim \vec{n}$ but leaves the total number of dual giant gravitons unrestricted. The ensemble is then left to select its own, optimal number of dual giant gravitons.

2. The analysis of Sec. 4.2 applies when one wishes to fix the total momentum of the dual giant gravitons to $\vec{P} \sim \vec{n}$ and the total number of dual giant gravitons to M. The previous expressions are modified via eq. (4.35). Several subcases are distinguished depending on the relation between M and $M_{\text{crit}}(\vec{P})$, eq. (4.41):

   2.1 If $M \leq M_{\text{crit}}(\vec{P})$ then eq. (4.34) sets the parameter α in a simple manner. In this case M can be thought of as fixing the *exact* number of dual giant gravitons, or the *maximal* number of dual giant gravitons.

   2.2 If $M > M_{\text{crit}}(\vec{P})$ fixes the *maximal* number of dual giant gravitons, the results of Sec. 4.2.2 apply. In that case, the number of dual giants that maximizes entropy equals $M_{\text{crit}}(\vec{P})$.

   2.3 If $M > M_{\text{crit}}(\vec{P})$ fixes the *exact* number of dual giant gravitons, the results of Sec. 4.2.3 apply.

4.4 Summary: The universal features of heavy operators

In all the theories we have considered, multi-trace operators and their single-trace factors are charged under three $U(1)$s. We have shown that for a given total charge $\vec{n}$, the distribution of charges of single-trace factors under a certain $U(1)$ is universal. This $U(1)$ is selected by a function $f(\vec{n})$ on the dual toric cone which measures the minimal volume in the cone cut out by a plane through $\vec{n}$. Given a triplet of charges $\vec{m}$, the charge of this particular

$U(1)$ is computed by the inner product $t(\vec{m}) = (\vec{m}, \vec{\nabla} f(\vec{n}))$. Then the fraction of single trace factors carrying U(1) charge $c_1 |\vec{n}|^{1/(d+1)} \leq t(\vec{m}) \leq c_2 |\vec{n}|^{1/(d+1)}$ for any constants c_1 and c_2 will be universal. The distribution of charges under the two residual $U(1)$s is not universal. In addition the total number of traces in a heavy multi-trace operator is proportional to $t(\vec{n})^{d/(d+1)}$. The proportionality factor depends only on the dimension d of the toric variety.

One concern about this result is that generic multi-trace operators may not be orthogonal and hence we may wonder whether an orthogonal basis enjoys the above universality properties. To examine this, we can imagine starting with one of the above operators and then systematically producing an orthogonal basis by a procedure like Gram-Schmidt. By the arguments given above, almost all the summands appearing in the orthogonal linear combinations will have the same trace structure. In this way, it appears that the universality will extend to an orthogonal basis. In any case, the dual giant graviton interpretation is free of this caveat. In that case, the universal properties include: (a) the number of dual giants in a typical state with total momentum $\vec{P}$, and (b) the fraction of the giants carrying a fixed amount of momentum around a particular cycle denoted $\sigma_{\vec{\nabla} f(\vec{P})}$.

5   Dual black hole geometries

In Sec. 3 we have enumerated heavy scalar mesonic BPS operators with a given charge vector $\vec{n}$. The structure of such operators exhibits many universal features, which were described in Sec. 4, either in the trace basis or using the dual giant graviton interpretation. The AdS/CFT correspondence anticipates that the dual description of such states is in terms of black hole geometries asymptotic to AdS_5. We now turn to reinterpret our previous results in terms of black hole physics.

5.1   Dual black holes have vanishing horizons

Here we argue that the dual black hole geometries have semi-classically vanishing horizons. Since by the Bekenstein relation the area is proportional to the entropy, $S = A/(4G_N)$, in our case we have

$$S_{\mathrm{grav.}} \sim \frac{\mathrm{Vol}(X)}{l_p^5} \frac{\rho_h^3}{l_p^3}, \tag{5.1}$$

where ρ_h is the radius of the horizon and $\mathrm{Vol}(X)$ is the volume of the transverse Sasaki–Einstein manifold X. This volume has been computed in [15], and is proportional to the volume of the 5-sphere as

$$\frac{\mathrm{Vol}(X)}{\mathrm{Vol}(S^5)} = \frac{a_{\mathcal{N}=4}}{a_{\mathcal{N}=1}} \equiv h(a_i), \tag{5.2}$$

where the constant of proportionality, $h(a_i)$, is the ratio of the central charges of the two dual SCFTs. It was shown in [9] that the volume of X is proportional to the volume of the

polytope Δ in the dual toric cone $\mathcal{C}^*$ bounded by the plane $2(\vec{b}, \vec{n}) = 1$:

$$\text{Vol}(X) = 6(2\pi)^3 \text{Vol}(\Delta) = 2(2\pi)^3 f((0,0,\tfrac{1}{6})) \,. \tag{5.3}$$

The second equality follows from the discussion above eq. (3.21). As $f_{S^5}((0,0,\tfrac{1}{6})) = \tfrac{1}{48}$, we have:

$$h(a_i) = 48 f((0,0,\tfrac{1}{6})) \,. \tag{5.4}$$

Using the relation between string length and Planck length, $l_p/l_s \sim g_s^{1/4}$, and the volume of the 5-sphere, $\text{Vol}(S^5) \sim (g_s N)^{5/4} l_s^5$, we solve for the horizon radius in string units as

$$\left(\frac{\rho_h}{l_s}\right)^3 \sim \left(\frac{l_p}{l_s}\right)^3 \frac{l_s^5}{\text{Vol}(X)} \left(\frac{l_p}{l_s}\right)^5 S_{\text{grav.}} \sim \frac{g_s^2 S_{\text{grav.}}}{(g_s N)^{\frac{5}{4}} h(a_i)} \sim \frac{(g_s N)^{\frac{3}{4}}}{h(a_i)} \frac{S_{\text{grav.}}}{N^2} \,. \tag{5.5}$$

This indicates that the radius of the horizon is nonzero in string units only if the entropy of the black hole scales as N^2 or faster, where N is the number of D-branes giving rise to the SCFT.

Naively, one would expect the dual geometries to correspond to black hole microstates once the conformal dimension is of the order N^2. This is because in other contexts black holes have been described in terms of a collection of N D-branes, each with conformal dimension of the order N [16]. These states do not have macroscopic horizons, however. To see this, consider any lattice site $\vec{n}$ in the dual toric cone whose conformal dimension is Δ. The volume of any pyramid cut out of the dual toric cone with a plane through $\vec{n}$ will grow as $|\vec{n}|^d$. Therefore $f(\vec{n}) \propto N^{2d}$ and by eq. (3.20):

$$S(\vec{n}) \propto N^{\frac{2d}{d+1}} = N^{2-\frac{2}{d+1}} \ll N^2 \,. \tag{5.6}$$

We conclude that the entropy never grows sufficiently fast to produce a horizon.

One might object that the above argument starts out treating N as a large but finite parameter while the calculations leading to eq. (3.20) assumed infinite N. The latter statement is an immediate consequence of working with dual toric *cones*, which extend along infinite rays. By contrast, in theories defined on finite stacks of D-branes, the ring of BPS operators will be subject to some non-trivial relations, due to the fact that for a rank N matrix, the operator $\text{Tr}(X^{N+1})$ can be written in terms of lower dimensional traces $\text{Tr}(X), \ldots, \text{Tr}(X^N)$. These relations are generated by Newton's identities applied to minimal loop operators and begin to kick in at distances of order N away from the tip of the cone. As a result, lattice points with $|\vec{n}| \gtrsim N$ in general fail to produce algebraically independent trace factors. We conclude that a finite N may be thought of as defining a truncation of the cone, so that all trace factors (partition summands) must fall within a rough distance N of the tip.

Happily, below eq. (4.32) we argued that, in almost all partitions, almost all summands satisfy $|\vec{m}| \propto |\vec{n}|^{\frac{1}{d+1}} \propto N^{\frac{2}{d+1}}$, so that $|\vec{m}| \ll N$ for $d > 1$. Therefore, a generic partition does not see the truncation by finite N. This establishes the consistency of the argument leading to (5.6). As an extra observation, notice that the inequality (5.6) is improved as d increases.

Finite horizons: Equation (5.5) tells us how the entropy of a black hole solution should scale for the black hole to have a macroscopic horizon. If we choose our conformal dimension to scale as $\Delta \sim N^\gamma$, we see that for a macroscopic horizon we need

$$N^2 \sim S \sim V^{\frac{1}{d+1}} \sim \Delta^{\frac{d}{d+1}} \sim N^{\frac{\gamma d}{d+1}} \quad \Rightarrow \quad \gamma = \frac{2(d+1)}{d} \rightarrow \frac{8}{3} \text{ for } d = 3. \qquad (5.7)$$

Thus the states of interest to us have conformal dimensions $\Delta \sim N^{8/3}$. Luckily, this is still not large enough to invalidate the argument above: in almost all partitions almost all summands satisfy $|\vec{m}| \sim |\vec{n}|^{\frac{1}{d+1}} \sim N^{\frac{\alpha}{d+1}} \sim N^{2/3}$, so that $|\vec{m}| \ll N$. It is interesting to note that γ decreases as d increases in keeping with the fact that less supersymmetry makes it easier to develop a horizon.[13]

Gravity duals of heavy operators: For states carrying non-vanishing R-charge in the superconformal field theory, the dual metrics were given in [17], who used the consistent truncation discovered in [18]. This R-charge is realized in supergravity by turning on angular momentum along the cycle defined by the Reeb vector. Denoting by ∂_ϕ the Killing vector field along the Reeb vector, the metric reads

$$ds^2 = -\frac{1}{4}H^{-2}F dt^2 + H[F^{-1}dr^2 + r^2 ds_{S^3}^2] + ds_Y^2 + (d\phi + A)^2, \qquad (5.8)$$

where Y is a four dimensional Kähler–Einstein manifold, and

$$
\begin{aligned}
H &= 1 + \frac{q}{r^2}, \\
F &= 1 + r^2 H^3, \\
A &= \frac{1}{2}H^{-1}dt\,.
\end{aligned}
\qquad (5.9)
$$

The gauge field A is responsible for the non-vanishing R-charge. These metrics have manifestly vanishing horizons, in agreement with our field theory counting and stretched horizon considerations. They carry only R-charge and are not charged under any extra U(1)s. This is equivalent to choosing our charge vector $\vec{n}$ to point in the z-direction (in the standard presentation), as dictated by (3.23).

For $\mathcal{M} = \mathbb{C}^3$, (singular) supersymmetric configurations with vanishing horizons have been known to exist for any value of the three U(1) R-charges, as long as the system remains BPS [19]. This statement matches our observations for any charge vector $\vec{n}$.

Since our methods and results apply to general toric varieties $\mathcal{M}$ with arbitrary U(1) charges turned on, any comparison with gravity would require the addition of these extra quantum numbers (nonzero flavor charges). To our knowledge such solutions have not been written down in the literature. We claim that the relevant geometries, when discovered, will be characterized by vanishing horizons.

---

[13] It is unclear to us whether such heavy operators will have a classical spacetime description in terms of an asymptotically $AdS_5 \times S^5$ metric, or whether this asymptotics will be modified.

6   Discussion

In this paper we developed a geometric way of counting scalar mesonic operators in $\mathcal{N} = 1$ toric quiver gauge theories based on the one-to-one correspondence between (equivalence classes of) gauge invariant operators and lattice points in the corresponding dual toric cone. This correspondence also allowed the recent development of the so-called plethystic program for counting the same quantities [1].

Our geometric considerations allowed us to analyze the structure of mesonic operators in the large charge limit using statistical arguments. This was accomplished by working with the appropriate partition functions (ensembles), and realizing that the set of states having the same occupation numbers form planar surfaces in the dual toric cone, inducing a natural grading on it. This connection allowed us to find the direction in the dual toric cone that had the most rapid growth of entropy.

In the large charge limit, the grading becomes a continuous variable y. We were able to use this to encode the structure of gauge invariant operators in terms of curves $x_d(y)$, whose properties only depend on the dimension d of the initial toric variety.[14] Here, $x_d(y)$ stands for the ratio of traces in a given multi-trace operators having grading value $\tilde{y} < y$. Similar mathematical functions control the distribution of all $U(1)$ charges among the traces of the heavy multi-trace operator.

Our statistical analysis shows that there exists a universal structure, shared by almost all heavy operators. In this sense, given an arbitrary constraint like fixed R-charge, there exists a typical state close to which almost all other states lie; these can be thought of as master states in the field theory. This provides a generalization, for any $\mathcal{N} = 1$ toric quiver gauge theory, of the results and philosophy reported in [13] for the half-BPS sector of $\mathcal{N} = 4$ SYM.

We mainly worked on the field theory side, and according to the AdS/CFT duality appropriate combinations of these operators are expected to be dual to microstate geometries on the gravity side. Unfortunately, the exact form of these geometries is not known for a general quiver.[15] Should these geometries be discovered in the future, our methods could be used to analyze the emergence of semi-classical gravity from the fundamental microstates in the spirit of [21].[16]

Even if we would know the explicit candidate microstate geometries, we know that their coarse-grained description would be interpreted in terms of distributions of giant gravitons or dual giants in $\mathrm{AdS}_5 \times X$. All our results can actually be reformulated in terms of dual giants

---

[14] In other words, the details about the precise nature of the toric variety are suppressed by negative powers of the charge, or equivalently, are suppressed in N.

[15] Recently, for the special case where the corresponding toric variety is $\mathbb{C}^3$, the equations describing the moduli space of such candidate microstate geometries were constructed in [20].

[16] Some recent work in the literature concerns the emergence of locality and spacetime from a study of the strong coupling dynamics of the gauge theory dual to the conifold [22]. It would be of interest to apply these techniques both to our heavy operators and to more general $\mathcal{N} = 1$ setups.

due to the isomorphism of Hilbert spaces discussed in Section 2.4.[17] Since our universality conclusions also apply in the description in terms of dual giant gravitons, this strongly suggests that the physical picture of black hole microstates advocated in [13] will also hold for all the systems described in this paper.

We have only worked at a classical level, and giants and dual giants are quantum mechanical objects. Thus, to establish the validity of our analysis, we need to show that the wavefunction of the configuration of D-branes is strongly localized, indicating that the system has a classical description. We established this localization for the case of giant gravitons on S^5 in appendix B and expect it to hold in a general setting.

In Section 5 we showed that to produce a macroscopic horizon, we would have to consider BPS mesonic states with conformal dimensions of at least of order $N^{8/3}$, for the case of a three dimensional toric variety, i.e., for string theory on $AdS_5 \times X$. It would be interesting to understand what these states look like on the gravity side, and why such large conformal dimensions are needed to create horizons. Naively one would expect a black hole to arise from a collection of $\mathcal{O}(N)$ D-branes and thus have a conformal dimension $N \cdot N \sim N^2 \ll N^{8/3}$. However, whatever the gravitational description, the structure of these states can be studied using our methods, barring a breakdown of the canonical ensemble itself.[18]

We would also like to point out that the case of a four (complex) dimensional toric variety might be interesting to study. In this case, the conformal dimension required to produce a macroscopic horizon is smaller, $N^{5/2}$, and the field theory is simpler. This is because increasing the (real) dimension of the toric variety by two, correspondingly decreases the dimension of the transverse Minkowski space by two, and after the near horizon limit this yields string theory on $AdS_3 \times \tilde{X}$, where $\tilde{X}$ is is the seven-dimensional base of the toric variety. This is naturally expected to be dual to a $(1 + 1)$-dimensional CFT.

Finally, we argued that even though the trace basis is not orthogonal for large values of the U(1) charges, the typicality we found would also be present in an orthogonal basis. However, it would be interesting to work explicitly with such an orthogonal basis, analogous to the basis of Schur polynomials for the half-BPS sector of $\mathcal{N} = 4$ super-Yang–Mills [23]. Such a basis was recently provided in [24] for the chiral ring of $\mathcal{N} = 4$ super-Yang–Mills. It would be interesting to extend that analysis and techniques to chiral rings of arbitrary $\mathcal{N} = 1$ superconformal field theories.

We expect that last point to be relevant for a comparison with gravity. This is because a generic heavy multi-trace chiral operator has no natural giant graviton interpretation [21] and we already know that Schur polynomials played a crucial role in matching the analysis of typicality in gauge theory with gravity [13].

---

[17] As discussed in appendix C, the existence of the identity between partition functions (2.13) suggests that a similar interpretation in terms of giants should also be possible, and would be more naturally formulated in terms of fermions.

[18] The ensemble might conceivably break down due to a Hagedorn-like growth in the number of states; it might be interesting to study this possibility further.

A Exact multiplicities of operators with irrational R-charges

In Section 3.1 we showed that the combined entropy of operators with co-planar charge vectors $\vec{n}$ is a function (eq. (3.11)) of the volume which the plane cuts out of the dual toric cone. The simplest application of this statement is to evaluate the total entropy of all operators of fixed R-charge R_0. The charge vectors satisfying this constraint live on the plane

$$(\vec{b}, \vec{n}) = \frac{3}{2}R_0 \,. \tag{A.1}$$

The volume of $\mathcal{C}^*$ bounded by the plane determines the total entropy via eq. (3.11).

The above statement is valid in the following two cases:

- When the Reeb vector $\vec{b}$ contains only one $\mathbb{Z}$-linearly independent component,

- When one wishes to impose (A.1) up to some small finite accuracy ϵ.

Suppose, however, that among the components of the Reeb vector there are $k > 1$ $\mathbb{Z}$-linearly independent ones. Denote them by r_i, $i = 1, \ldots, k$. One example of that is dP_1, where $\vec{b} = (0, 4 - \sqrt{13}, 3)$ and $4 - \sqrt{13}$, 3 are $\mathbb{Z}$-linearly independent. Suppose further that one is interested in constraining the R-charge at *exactly* R_0. We may decompose R_0 and $\vec{b}$ into summands proportional to r_i:

$$\begin{aligned} \vec{b} &= r_1 (b_1^1, b_2^1, b_3^1) + \ldots + r_k (b_1^k, b_2^k, b_3^k) \\ R_0 &= r_1 R_0^1 + \ldots + r_k R_0^k \,. \end{aligned} \tag{A.2}$$

If no decomposition of R_0 is possible, then no state with $R = R_0$ exists and computing the entropy is meaningless. Otherwise, the constraint (A.1) decomposes into k independent ones:

$$(\vec{b^i}, \vec{n}) = \frac{3}{2}R_0^i \qquad i = 1, \ldots, k \,. \tag{A.3}$$

Therefore the locus of charge vectors *exactly* matching R_0 is given by the region of intersection of $\mathcal{C}^*$ and k planes (A.3). In other words, it is the section of a certain $(d - k)$-hyperplane contained in the dual toric cone.

For $d = 3$, three cases are distinguished:

1. $k = 1$. The locus $R = R_0$ is a plane. The combined entropy is determined by the volume of $\mathcal{C}^*$ contained under the plane as explained in Section 3.1.

2. $k = 3$. The locus $R = R_0$ is a point. The entropy is determined by the minimal volume of $\mathcal{C}^*$ that may be cut out with one plane through the point $R = R_0$. This was explained in Section 3.2.

3. $k = 2$. The locus $R = R_0$ is a line. This case, along with all others with $1 < k < d$, is treated in the next subsection.

A.1 Multiplicities of collinear vectors

The argument of Section 3.2 is readily adapted to $1 < k < d$. The locus of points of interest is a $(d-k)$-hyperplane satisfying k equations (A.3). Consider the family of $(d-1)$-hyperplanes $H_{\vec{s}}$ containing the locus $R = R_0$. Here $\vec{s}$ is the normal to the hyperplane, which is specified by $k-1$ free parameters. In particular, $\vec{s}$ is a linear combination of the vectors $\vec{b}^i$ whose normalization is immaterial and may be scaled to 1.

For each such $\vec{s}$, consider the family of $(d-1)$-planes parallel to it and proceed as in Section 3.1. The total entropy of the points $\{R = R_0\}$ is bounded from above by

$$S(R_0) \leq \min_{\vec{s} = \sum_{i=1}^{k} a_i \vec{b}^i} S(p_{\vec{s}}). \qquad (A.4)$$

Here $S(p_{\vec{s}})$ denotes the total multiplicity of all charge vectors contained in $p_{\vec{s}}$, which may be obtained from eq. (3.11). Assume that every $(d-k)$-hyperplane $\{R = R_0'\}$ in $p_{\vec{s}_{\min}(R_0)}$ has its own minimal $\vec{s}_{\min}(R_0')$. Since the region $\{R = R_0'\}$ is contained in $p_{\vec{s}_{\min}(R_0)}$, its minimum must be strictly smaller than the entropy of the $(d-1)$-plane $p_{\vec{s}_{\min}(R_0)}$. This applies to every locus $\{R = R_0' \neq R_0\}$, which implies that:

$$S(R_0) \approx \min_{\vec{s} = \sum_{i=1}^{k} a_i \vec{b}^i} S(p_{\vec{s}}). \qquad (A.5)$$

This equation applies to all $1 \leq k \leq d$ and naturally generalizes eq. (3.13).

As k grows, one is able to derive more information from a single exact measurement of the R-charge. Such successive specifications narrow down the microcanonical ensemble of states $\{R = R_0\}$, which should result in a decrease of the multiplicities computed in eq. (A.5). We may see that this is indeed the case from the schematic relationship

$$\begin{aligned} S(R_0)|_{k=d} &\approx \min_{\vec{s} = \sum_{i=1}^{d} a_i \vec{b}^i} S(p_{\vec{s}}) \\ \leq S(R_0)|_{k=d-1} &\approx \min_{\vec{s} = \sum_{i=1}^{d-1} a_i \vec{b}^i} S(p_{\vec{s}}) \leq \dots \\ \leq S(R_0)|_{k=1} &= S(p_{\vec{b}}). \end{aligned} \qquad (A.6)$$

The multiplicities obtained from specifying the charge vector $\vec{n}$ with a growing number of constraints differ only in the domain of minimization in eq. (A.5). In particular, they are of the same order of magnitude.

41

B Mapping to the typical giant configuration

In Section 4.3 we interpreted our analysis as giving a typical configuration of dual giant gravitons. However, all these configurations are at heart quantum mechanical, and to analyze typicality we should verify that the wavefunction of the typical configuration is sharply peaked, thereby allowing one to associate it to a semiclassical collection of D-branes. In this appendix we will argue that this indeed is the case: the typical states constructed above can be associated to a typical configuration of giant gravitons on the gravity side. For simplicity, we will deal with giant gravitons on S^5; we expect the conclusions to be valid in a more general setting as well.

It was shown by Mikhailov [25] and Beasley [11] that these brane configurations can be given in terms of zero-loci of polynomials of the form

$$P(z_1, z_2, z_3) = \sum_{\vec{n}} c_{n_1 n_2 n_3} z_1^{n_1} z_2^{n_2} z_3^{n_3}, \tag{B.1}$$

where $\vec{n}$ runs over $\mathbb{N}^3$. The worldvolumes of the branes are given by the intersection of the surface $P(\vec{z}) = 0$ with the unit S^5 in $\mathbb{C}^3$, where the S^5 is identified with the one in $AdS_5 \times S^5$. The phase space of brane configurations is thus spanned by $\{c_{n_1 n_2 n_3}\}$ and is topologically $\mathbb{CP}^\infty$.

This space was quantized in [26] using geometric quantization. First one defined a new set of coordinates that eliminated the pathological regions in coordinates $\{c_{n_1 n_2 n_3}\}$, i.e., eliminated polynomials that don't intersect the unit S^5 and identified polynomials that have the same intersection with the S^5. The new coordinate system is given as

$$w_{n_1 n_2 n_3} = f_{|n_1 + n_2 + n_3|}(\vec{c}) c_{n_1 n_2 n_3}, \tag{B.2}$$

where $f_{|n_1 + n_2 + n_3|}$ is a smooth function. Upon quantization the Hilbert space of brane configurations was found to be the space of degree N holomorphic polynomials in $w_{n_1 n_2 n_3}$, which is isomorphic to the Hilbert space of N free bosons in a three dimensional harmonic oscillator, and therefore has the partition function

$$Z = \prod_{j=1}^{N_c} \frac{1}{(1 - e^{-\beta j})^{\frac{1}{2} j(j+1)}}. \tag{B.3}$$

Above, we've restricted the highest excitation any particle can have to be given by the constant N_c; physically this corresponds to fixing the the number of giant gravitons [13]. This is because the highest excitation gives the degree of the polynomial $P(z_1, z_2, z_3)$ and therefore the maximal number of D-branes. In the following we'll also work in the high temperature regime, $\beta \to 0$.

We can now write down the wave function of the typical state. Since the energy levels factorize, we have

$$\Psi^{\text{typical}}(\vec{w}) = \prod_{j=0}^{N_c} \psi_j(\vec{w}), \tag{B.4}$$

42

where ψ_j is the contribution from particles with energy j to the total wavefunction. Since the wave function has to be symmetric both under the exchange of particles and under the exchange of dimensions, we can write

$$\psi_j(\vec{w}) = \left[\sum_{\substack{n_x,n_y,n_z=0 \\ n_x+n_y+n_z=j}}^{j} w_{n_x,n_y,n_z} \right]^{k_j}. \tag{B.5}$$

Since the moduli space is $\mathbb{CP}^\infty$, the coordinates have to satisfy $\sum_{n_x,n_y,n_z} |w_{n_x,n_y,n_z}|^2 = 1$. If we define the contribution from each energy level j as R_j^2, we can write this condition as

$$\sum_{\substack{n_x,n_y,n_z=0 \\ n_x+n_y+n_z=j}}^{j} |w_{n_x,n_y,n_z}|^2 = R_j^2, \quad \text{with} \sum_{j=0}^{N_c} R_j^2 = 1. \tag{B.6}$$

For any given R_j, we know that the maximum of $|\sum_{\substack{n_x,n_y,n_z=0 \\ n_x+n_y+n_z=j}}^{j} w_{n_x,n_y,n_z}|$ occurs when all the w's are equal, and since the number of states at energy level j is $\binom{j+2}{2}$, we see that the correct value is

$$w_{n_1 n_2 n_3} \equiv w_j = \sqrt{\frac{R_j^2}{d_j}}, \quad \forall\, n_1 + n_2 + n_3 = j. \tag{B.7}$$

(Up to an overall phase that is not relevant to us.) Thus at the maximum the wavefunction can be written as

$$\Psi(\vec{w}) = \prod_{j=0}^{N_c} \left[\binom{j+2}{2} w_j \right]^{k_j} = C \prod_{j=0}^{N_c} R_j^{k_j}, \tag{B.8}$$

where the normalization constant C is not important and will be dropped. We wish to maximize $|\Psi|^2$ with the constraint $\sum R_j^2 = 1$, and to do this we eliminate R_0 by solving the constraint, yielding

$$|\Psi(\vec{w})|^2 = \left(1 - \sum_{k=1}^{N_c} R_k^2 \right)^{k_0} \prod_{l=1}^{N_c} R_l^{2k_l}. \tag{B.9}$$

After some algebra one finds the maximum of this at

$$R_j = \sqrt{\frac{k_j}{N}}, \quad \forall\, j, \tag{B.10}$$

which by construction satisfies $\sum R_j^2 = 1$. This is the only local extremum, and since the wavefunction vanishes on the 'edges' where $w_j = 0$ for some j, this is also the global maximum.

Finally, we compute the second derivative of the wavefunction at the maximum. After some algebra this yields

$$\frac{1}{|\Psi(\vec{w})|^2} \frac{\partial^2 |\Psi(\vec{w})|^2}{\partial R_j \partial R_i} \bigg|_{max} = -4N \left(\frac{\sqrt{k_i k_j}}{k_0} + \delta_{ij} \right). \tag{B.11}$$

Since in the large temperature limit $\beta \to 0$ the free energy is minimized when the entropy is maximized, we see that for the typical state the particles are evenly distributed among all possible states[19] , and therefore the number of particles on energy level j is $k_j \propto \binom{j+2}{2}$. Thus we see that in the limit $N \to \infty$ the wavefunction is sharply peaked around the maximum, and we can associate the typical state with the location of the maximum in the phase space, $\vec{w}^{max}$. The map (B.2) then guarantees that there exists a corresponding point $\vec{c}^{max}$ specifying the typical configuration of giant gravitons. We expect this configuration to correspond to the superstar [16], but have been unable to verify this as the explicit form of the funtion $f_{|n_1+n_2+n_3|}(\vec{c})$ in (B.2) is not known.

C   Limiting Curves and Amoebae?

There have recently been developments in topological strings using the statistical physics of so-called melting crystals [27, 28]. Analyses of typical states in black hole physics have involved the use of similar statistical mechanics techniques. In this brief appendix we would like to comment on the similarities and differences between the two and make some speculative remarks.

In the melting crystal studies one considers geometric quantization of a *single particle* in $\mathbb{C}^m$. Its spectrum is that of a harmonic oscillator in m dimensions, and as such, the associated partition function is related to a classical partition function. For example, for $\mathbb{C}^3$, there is a one-to-one map between quantum harmonic oscillator states and 3-D Young tableaux. If we associate each tableaux with a distribution of boxes in an octant of $\mathbb{R}^3$, the statistical mechanics provides the limiting shape for the boundary of the crystal as a function of the string coupling, which plays the role of the temperature in this set-up.

This discussion is conceptually very reminiscent of the derivation of the typical state in the half-BPS sector of $\mathcal{N} = 4$ SYM. There is a one-to-one correspondence between N-*particle* fermionic quantum states in a 1-dimensional harmonic oscillator and 2-dimensional Young tableaux. Statistical mechanics and a large N limit allow the derivation of a limit shape $y(x)$ which describes the average excitation (y) of the particle x.

Though the techniques are the same, the physics looks rather different. The plethystic methods and the geometric quantization of the classical moduli space of dual giants provide a clue as to where a relation may exist. Let us consider the isomorphism, which is a cornerstone of the plethystic program:

$$g_N(t, \mathcal{M}) = g_1(t, \mathcal{M}^N/S_N) . \tag{C.1}$$

This states that the number of mesonic scalar chiral primary gauge invariant multi-trace operators constructed out of building blocks that define $\mathcal{M}$ is equal to the number of single trace operators in a different manifold, the symmetric product $\mathcal{M}^N/S_N$. In terms of dual giant gravitons, this has a very natural interpretation: the Hilbert space of N dual giants is equivalent to the symmetric space of the Hilbert space spanned by a single giant, which is

---

[19] This is also easy to derive from (B.3) more rigorously.

the set of holomorphic functions in $\mathcal{M}$. Therefore, (C.1) provides a bridge between partition functions of N *particles* and partition functions of a *single particle* in a different space.

Consider the particular case of $\mathcal{M} = \mathbb{C}$. The Hilbert space of a single particle is that of a harmonic oscillator in one dimension. When we consider the Hilbert space of a single particle in $\mathbb{C}^N/S_N$, all quantum numbers in each of the copies appearing in the symmetric product have to be different: this is effectively implementing the Pauli exclusion principle, and so we conclude that we are equivalently dealing with N *fermions* in a one dimensional harmonic oscillator. The limiting curve, exhibited in eq. (44) of [13], is given by

$$ae^{\beta x} + be^{-\beta y} = 1 \ , \qquad a = e^{-\beta N}, \quad b = 1 - a \tag{C.2}$$

and reproduces the curve $x_1(y)$ of eq. (4.29) up to a linear re-definition of coordinates. Inspecting Section 4.1 of [28] we see the emergence of (C.2) therein. Equivalently, in the language of [29], (C.2) is the boundary of the amoeba of $\mathbb{C}^3$, which, in turn, is equivalent to the limiting shape of constructing three-dimensional Young tableaux.

We can now understand the space where the limiting curve $y(x)$ lives. Indeed, x can be understood as parameterizing the copy x in the symmetric product $\mathbb{C}^N/S_N$ (or the particle x in the dual giant language) whereas y is just describing the excitation of that copy (particle). In the semiclassical limit x is a continuum variable, and we obtain a curve on a two dimensional plane. This curve describes a single particle living not in $\mathbb{C}^2$, but rather in the symmetric product $\mathbb{C}^N/S_N$ with $N \to \infty$.

To recapitulate, we have that (1) the curve of typicality of half-BPS states of $\mathcal{N} = 4$ SYM identifies with (2) the limiting curve of the topological A-model on $\mathbb{C}^3$. We point out that the underlying geometries of the two differ: the fundamental generating function (i.e., for the single-trace operator) of (1), in the language of the plethystic program, is the Hilbert series for $\mathbb{C}$ while the curve in (2) is the amoeba for $\mathbb{C}^3$. Nevertheless, the emergence of the same curve in two different counting problems suggests that there may be a deeper connection, possibly persisting to other geometries, and hence other $\mathcal{N} = 1$ theories, which we should explore.

References

[1] S. Benvenuti, B. Feng, A. Hanany and Y. H. He, "Counting BPS operators in gauge theories: Quivers, syzygies and plethystics," [arXiv:hep-th/0608050].
B. Feng, A. Hanany and Y. H. He, "Counting gauge invariants: The plethystic program," JHEP **0703**, 090 (2007) [arXiv:hep-th/0701063].

[2] A. Butti, D. Forcella and A. Zaffaroni, "Counting BPS baryonic operators in CFTs with Sasaki-Einstein duals," JHEP **0706**, 069 (2007) [arXiv:hep-th/0611229].

[3] D. Forcella, A. Hanany and A. Zaffaroni, "Baryonic generating functions," [arXiv:hep-th/0701236]. A. Butti, D. Forcella, A. Hanany, D. Vegh and A. Zaffaroni, "Counting Chiral Operators in Quiver Gauge Theories," [arXiv:0705.2771 [hep-th]].

[4] D. Martelli and J. Sparks, "Dual giant gravitons in Sasaki-Einstein backgrounds," Nucl. Phys. B **759**, 292 (2006) [arXiv:hep-th/0608060].

[5] A. Kehagias, "New type IIB vacua and their F-theory interpretation," Phys. Lett. B **435**, 337 (1998) [arXiv:hep-th/9805131].
I. R. Klebanov and E. Witten, "Superconformal field theory on threebranes at a Calabi-Yau singularity," Nucl. Phys. B **536**, 199 (1998) [arXiv:hep-th/9807080].
B. S. Acharya, J. M. Figueroa-O'Farrill, C. M. Hull and B. J. Spence, "Branes at conical singularities and holography," Adv. Theor. Math. Phys. **2**, 1249 (1999) [arXiv:hep-th/9808014].
D. R. Morrison and M. R. Plesser, "Non-spherical horizons. I," Adv. Theor. Math. Phys. **3**, 1 (1999) [arXiv:hep-th/9810201].

[6] K. D. Kennaway, "Brane Tilings," Int. J. Mod. Phys. A **22**, 2977 (2007) [arXiv:0706.1660 [hep-th]].

[7] B. Feng, A. Hanany and Y. H. He, "D-brane gauge theories from toric singularities and toric duality," Nucl. Phys. B **595**, 165 (2001) [arXiv:hep-th/0003085].

[8] W. Fulton, "Introduction to Toric Varieties," Princeton University Press (1993).
H. Skarke, "String dualities and toric geometry: An introduction," [hep-th/9806059].
V. Bouchard, "Lectures on complex geometry, Calabi-Yau manifolds and toric geometry," [hep-th/0702063].

[9] D. Martelli, J. Sparks and S. T. Yau, "The geometric dual of a-maximisation for toric Sasaki-Einstein manifolds," Commun. Math. Phys. **268**, 39 (2006) [hep-th/0503183].

[10] D. Martelli and J. Sparks, "Toric geometry, Sasaki-Einstein manifolds and a new infinite class of AdS/CFT duals," Commun. Math. Phys. **262**, 51 (2006) [hep-th/0411238].

[11] C. E. Beasley, "BPS branes from baryons," JHEP **0211**, 015 (2002) [hep-th/0207125].

[12] G. Meinardus, "Asymptotische Aussagen über Partitionen," Matematische Zeitschrift **59** (1954) 388-398.
A. A. Actor, "Infinite products, partition functions, and the Meinardus theorem," J. Mathematical Physics, Vol 35,11, Nov. 1994, pp. 5749-5764.

[13] V. Balasubramanian, J. de Boer, V. Jejjala and J. Simón, "The library of Babel: On the origin of gravitational thermodynamics," JHEP **0512**, 006 (2005) [arXiv:hep-th/0508023].

[14] V. Balasubramanian, B. Czech, V. E. Hubeny, K. Larjo, M. Rangamani and J. Simón, "Typicality versus thermality: An analytic distinction," [arXiv:hep-th/0701122].

[15] D. Martelli, J. Sparks and S. T. Yau, "Sasaki-Einstein manifolds and volume minimisation," [arXiv:hep-th/0603021].

[16] R. C. Myers and O. Tafjord, "Superstars and giant gravitons," JHEP **0111**, 009 (2001) [arXiv:hep-th/0109127].

[17] J. P. Gauntlett, N. Kim and D. Waldram, "Supersymmetric AdS(3), AdS(2) and bubble solutions," JHEP **0704**, 005 (2007) [arXiv:hep-th/0612253].

[18] A. Buchel and J. T. Liu, "Gauged supergravity from type IIB string theory on Y(p,q) manifolds," Nucl. Phys. B **771**, 93 (2007) [arXiv:hep-th/0608002].

[19] K. Behrndt, A. H. Chamseddine and W. A. Sabra, "BPS black holes in N = 2 five dimensional AdS supergravity," Phys. Lett. B **442**, 97 (1998) [arXiv:hep-th/9807187].

[20] B. Chen *et al.*, "Bubbling AdS and droplet descriptions of BPS geometries in IIB supergravity," JHEP **0710**, 003 (2007) [arXiv:0704.2233 [hep-th]].

[21] V. Balasubramanian, B. Czech, K. Larjo, D. Marolf and J. Simon, "Quantum geometry and gravitational entropy," [arXiv:0705.4431 [hep-th]].

[22] D. Berenstein, "Strings on conifolds from strong coupling dynamics, part I," [arXiv:0710.2086 [hep-th]].
D. E. Berenstein and S. A. Hartnoll, "Strings on conifolds from strong coupling dynamics: quantitative results," [arXiv:0711.3026 [hep-th]].

[23] S. Corley, A. Jevicki and S. Ramgoolam, "Exact correlators of giant gravitons from dual N = 4 SYM theory," Adv. Theor. Math. Phys. **5**, 809 (2002) [arXiv:hep-th/0111222].

[24] T. W. Brown, P. J. Heslop and S. Ramgoolam, "Diagonal multi-matrix correlators and BPS operators in N=4 SYM", [arXiv:0711.0176].

[25] A. Mikhailov, "Giant gravitons from holomorphic surfaces," JHEP **0011**, 027 (2000) [arXiv:hep-th/0010206].

[26] I. Biswas, D. Gaiotto, S. Lahiri and S. Minwalla, "Supersymmetric states of N = 4 Yang-Mills from giant gravitons," [arXiv:hep-th/0606087].

[27] A. Okounkov, N. Reshetikhin and C. Vafa, "Quantum Calabi-Yau and classical crystals," [arXiv:hep-th/0309208].

[28] A. Iqbal, N. Nekrasov, A. Okounkov and C. Vafa, "Quantum foam and topological strings," [arXiv:hep-th/0312022].

[29] B. Feng, Y. H. He, K. D. Kennaway and C. Vafa, "Dimer models from mirror symmetry and quivering amoebae," [arXiv:hep-th/0511287].